indicated in each figure), and the reaction was stopped by placing the tubes on ice. The reaction tubes were not agitated. From each reaction tube, triplicate 5-μL aliquots were removed, then subjected to fluorescence spectroscopy and the mean of each triplicate determined. In the ThT solution, the concentration of NDGA and polyphenols examined in this study was diluted up to 1/200 of that in the reaction mixture. We confirmed that these compounds did not quench ThT fluorescence at the diluted concentration (data not shown).

Destabilization assay

Destabilization assay was performed as described by Ono *et al.* (2002b). Briefly, the reaction mixture contained 25 μM fresh fAβ(1–40) or fAβ(1–42), 0, 0.01, 0.1, 1, 10, or 50 μM NDGA or polyphenols, 1% DMSO, 50 mM phosphate buffer, pH 7.5, 100 mM NaCl, and 1% (wt/vol) polyvinyl alcohol (Wako Pure Chemical Industries Ltd) to avoid the aggregation of fAβ and the adsorption of fAβ onto the inner wall of the reaction tube during the reaction.

Triplicate 5 μL aliquots were mixed by pipette then subjected to fluorescence spectroscopy, 30 μL aliquots were put into PCR tubes. The reaction tubes were then transferred into a DNA thermal cycler. The plate temperature was elevated to maximal speed, starting at 4°C, and raised to 37°C. Incubation times ranged between 0 and 72 h (as indicated in each figure), and the reaction was stopped by placing the tubes on ice. The reaction tubes were not agitated during the reaction. From each reaction tube, 5 μL aliquots in triplicate were subjected to fluorescence spectroscopy and the mean of the three measurements was determined.

Cell Cultures and MTT assay

Cell cultures and MTT assay were performed as described by Yoshiike *et al.* (2001). Human embryonic kidney (HEK) 293 cells were grown in Dulbecco's modified Eagle's medium (DMEM) (Sigma, St Louis, MO, USA) containing 10% fetal bovine serum (HyClone, Logan, UT, USA) and incubated in a humidified chamber (85% humidity) containing 5% CO_2 at 37°C. A day prior to the fAβ treatment, the cell culture medium was replaced with serum-free DMEM, and the cells were plated onto a 96-well coated plate (Corning, NY, USA) at a final cell count of 20 000 cells/well.

Ten μM fAβ(1–40) were incubated with 0 or 0.2% DMSO, or 10 μM Myr + 0.2% DMSO at pH 7.5 at 37°C. ThT fluorescence was regularly monitored as described in Yoshiike *et al.* (2001). After 6 h, the incubation mixtures were added immediately to HEK 293 cell cultures. Cells were treated with a final concentration of 0 or 1 μM intact, DMSO-treated or Myr-treated fAβ(1–40) containing 0 or 0.02% DMSO, or 1 μM Myr + 0.02% DMSO, respectively, in serum-free DMEM for 2 h. MTT was then added to each well and the plate was kept in a CO_2 incubator for an additional 2 h. The cells were then lysed by the addition of a lysis solution (50% dimethylformamide, 20% SDS, pH 4.7) and were incubated overnight. The degree of MTT reduction in each sample was subsequently assessed by measuring absorption at 570 nm and at 37°C using a Bio Kinetics EL340 reader (Bio-Tek Instruments, Winooski, VT, USA). Background absorbance values, as assessed from cell-free wells, were subtracted from the absorption values of each test sample. Percentage of MTT reduction was calculated by taking the average from a condition with neither fAβ, Myr, nor DMSO as 100% in each experiment.

Other analytical procedures

Protein concentrations of the supernatants of the reaction mixtures after centrifugation were determined by the method of Bradford (1976) with a protein assay kit (Bio-Rad Laboratories, Inc., Hercules, CA). The Aβ1–40 solution quantified by amino acid analysis was used as the standard. Paired Student's *t*-test and linear least squares fit were used for statistical analysis. The effective concentrations (EC_{50}) were defined as the concentrations of NDGA or polyphenols to inhibit the formation or extension of fAβs to 50% of the control value, or the concentrations to destabilize fAβs to 50% of the control value. EC_{50} were calculated by the sigmoidal curve fitting of the data as shown in Figs 1(e), 2(f) and 4(e), using Igor Pro ver.4 (WaveMetrics, Inc., Lake Oswego, OR, USA).

Results

Effect of polyphenols on the kinetics of fAβ polymerization

As shown in Fig. 1(a-d), when fresh Aβ(1–40) or Aβ(1–42) was incubated at 37°C, the fluorescence of ThT followed a characteristic sigmoidal curve. This curve is consistent with a nucleation-dependent polymerization model (Jarrett and Lansbury 1993; Naiki *et al.* 1997). fAβ(1–40) and fAβ(1–42) stained with Congo red showed typical orange-green birefringence under polarized light (data not shown). When Aβ(1–40) was incubated with 10 and 50 μM Myr, Mor or Qur, no increase in the fluorescence was observed throughout the reaction (Fig. 1(a) and data not shown). A similar effect of Myr, Mor and Qur was observed with Aβ(1–42) (Fig. 1(b) and data not shown). When Aβ(1–40) was incubated with 10 and 50 μM Kmp, Cat or epi-Cat, the final equilibrium level decreased dose-dependently (Fig. 1 (c) and (d) and data not shown). A similar effect of Kmp, Cat and epi-Cat was observed with Aβ(1–42) (data not shown).

As shown in Fig. 2(a-d), when fresh Aβ(1–40) or Aβ(1–42) was incubated with fAβ(1–40) or fAβ(1–42), respectively, at 37°C, the fluorescence increased hyperbolically without a lag phase and proceeded to equilibrium much more rapidly than without seeds (compare Figs 1 and 2). This curve is consistent with a first-order kinetic model (Naiki and Nakakuki 1996). When Aβ(1–40) and fAβ(1–40) were incubated with polyphenols, the final equilibrium level decreased (Fig. 2a, 2c,d). A similar effect of polyphenols was observed for the extension of fAβ(1–42) (Fig. 2(b) and data not shown). At a constant fAβ(1–40) concentration, a perfect linearity was observed between the Aβ(1–40) concentration and the initial rate of fAβ(1–40) extension both in the presence and absence of Myr (Fig. 2e). This linearity is again consistent with a first-order kinetic model and indicates that at each Aβ(1–40) concentration, the net rate of fAβ(1–40) extension is the sum of the rates of polymerization and depolymerization (Naiki and Nakakuki 1996; Hasegawa *et al.* 2002). In the presence of 10 μM Myr, the slope of the

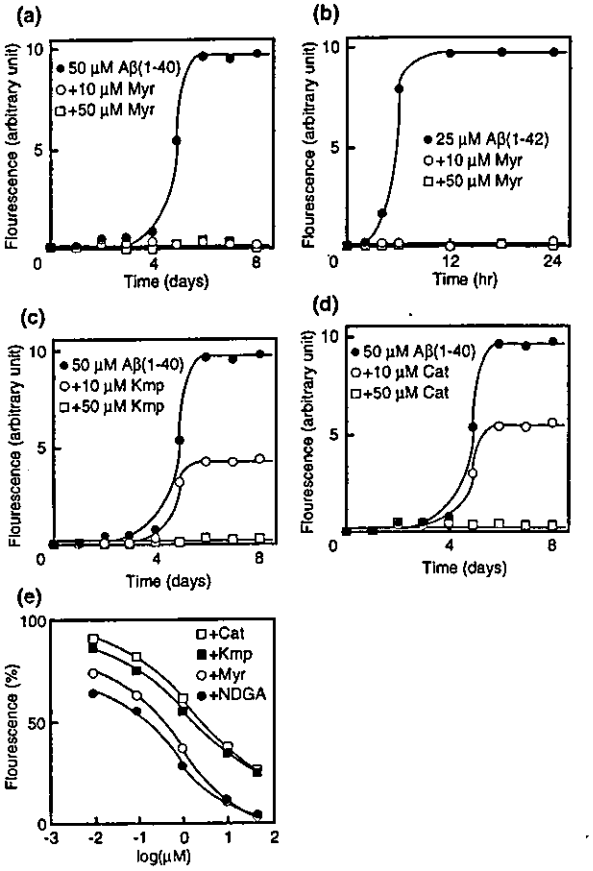

Fig. 1 (a-d) Effects of Myr (a, b), Kmp (c), and Cat (d) on the kinetics of fAβ(1–40) (a, c, d) and fAβ(1–42) (b) formation from fresh Aβ(1–40) and Aβ(1–42), respectively. The reaction mixtures containing 50 μM Aβ(1–40) (a, c, d) or 25 μM Aβ(1–42) (b), 50 mM phosphate buffer, pH 7.5, 100 mM NaCl, and 0 (●), 10 (○), or 50 μM (○) of Myr (a, b), Kmp (c), or Cat (d), were incubated at 37°C for the indicated times. Each figure is a representative pattern of 3 independent experiments. (e) Dose-dependent inhibition of fAβ(1–40) formation from fresh Aβ(1–40). The reaction mixtures containing 50 μM Aβ(1–40), 50 mM phosphate buffer, pH 7.5, 100 mM NaCl, and 0, 0.01, 0.1, 1, 10 and 50 μM NDGA (●), Myr (○), Kmp (■), or Cat (□) were incubated at 37°C for 7 days. Points represent means of three independent experiments. In all points, standard errors were within symbols. The average without compounds was regarded as 100%.

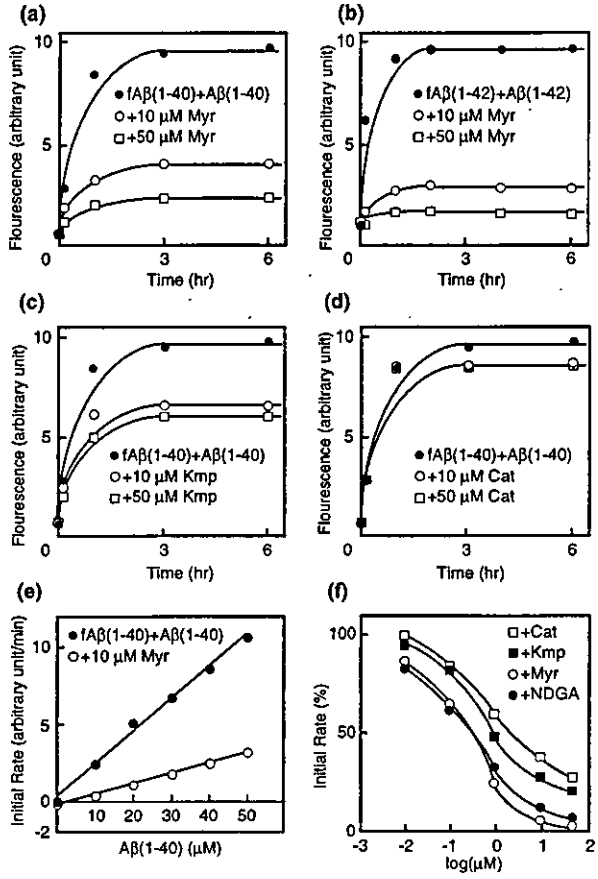

Fig. 2 (a-d) Effects of Myr (a, b), Kmp (c), and Cat (d) on the kinetics of fAβ(1–40) (a, c, d) and fAβ(1–42) (b) extension. The reaction mixtures containing 10 μg/mL (2.3 μM) sonicated fAβ(1–40) (a, c, d) or fAβ(1–42) (b), 50 μM Aβ(1–40) (a, c, d) or Aβ(1–42) (b), 50 mM phosphate buffer, pH 7.5, 100 mM NaCl, and 0 (●), 10 (○), or 50 μM (□) of Myr (a, b), Kmp (c), or Cat (d), were incubated at 37°C for the indicated times. Each figure is a representative pattern of 3 independent experiments. (e) Effect of Aβ(1–40) concentration on the initial rate of fAβ(1–40) extension in the presence (○) and absence (●) of Myr. The reaction mixtures containing 10 μg/mL (2.3 μM) sonicated fAβ(1–40), 50 mM phosphate buffer, pH 7.5, 100 mM NaCl, 0 (●) or 10 μM (○) Myr, and 0, 10, 20, 30, 40, and 50 μM Aβ(1–40), were incubated at 37°C for 1 h. Points represent means of three independent experiments. In all points, standard errors were within symbols. Liner least-square fit was performed for each straight line (R^2 = 0.998 and 0.994 for ○ and ●, respectively). (f) Dose-dependent inhibition of fAβ(1–40) extension. The reaction mixtures containing 10 μg/mL (2.3 μM) sonicated fAβ(1–40), 50 μM Aβ(1–40), 50 mM phosphate buffer, pH 7.5, 100 mM NaCl, and 0, 0.01, 0.1, 1, 10 and 50 μM NDGA (●), Myr (○), Kmp (■), or Cat (□) were incubated at 37°C for 1 h. Points represent means of three independent experiments. In all points, standard errors were within symbols. The average without compounds was regarded as 100%.

straight line decreased to about 3/10. The interpretation of this figure implicating the mechanism of the anti-amyloidogenic effect of Myr will be discussed later.

When fresh Aβ(1–40) was incubated with fAβ(1–40) at 37°C, clear fibril extension was observed electron-microscopically (Fig. 3b). However, 50 μM Myr completely inhibited the extension of sonicated fAβ(1–40) (Fig. 3a,c). Myr inhibited the extension of fAβ(1–42) (data not shown). Similarly, Mor, Qur and Kmp also inhibited the extension of fAβ(1–40) and fAβ(1–42) (data not shown).

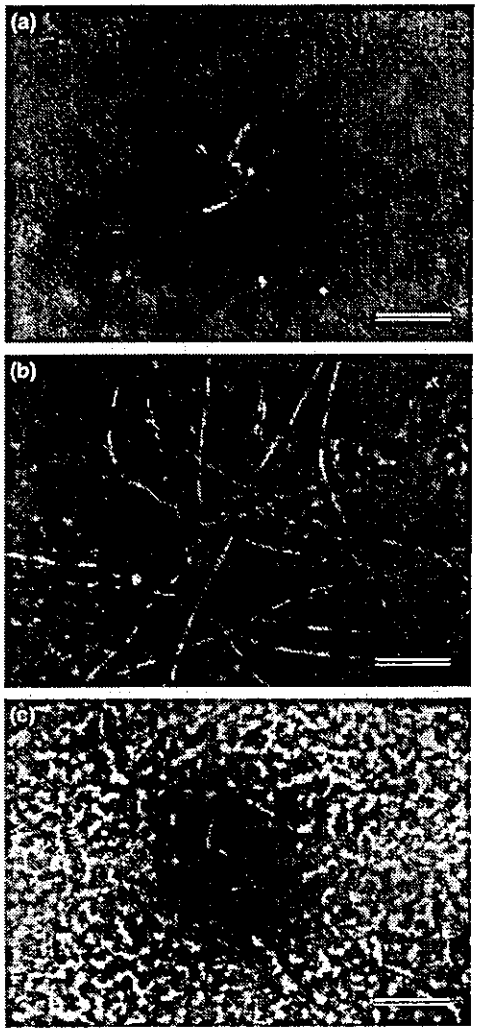

Fig. 3 Electron micrographs of extended fAβ(1–40). The reaction mixtures containing 10 μg/mL (2.3 μM) fAβ(1–40), 50 μM Aβ(1–40), 50 mM phosphate buffer, pH 7.5, 100 mM NaCl, and 0 (b) or 50 μM Myr (a, c), were incubated at 37°C for 0 (a), or 6 h (b, c). Scale bars indicate a length of 250 nm.

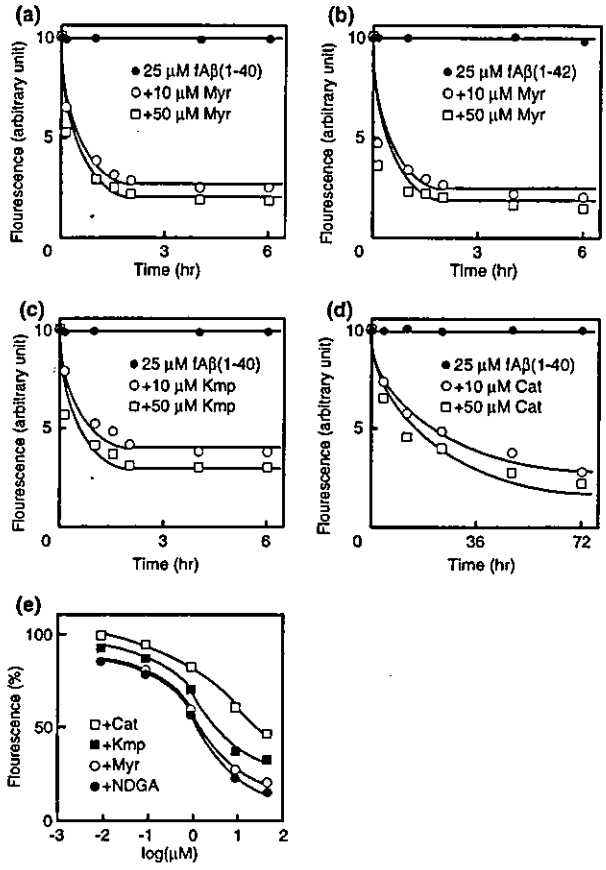

Fig. 4 (a-d) Effects of Myr (a, b), Kmp (c), and Cat (d) on the kinetics of fAβ(1–40) (a, c, d) and fAβ(1–42) (b) destabilization. The reaction mixtures containing 25 μM fAβ(1–40) (a, c, d) or fAβ(1–42) (b), 50 mM phosphate buffer, pH 7.5, 100 mM NaCl, and 0 (●), 10 (○), or 50 μM (□) of Myr (a, b), Kmp (c), or Cat (d), were incubated at 37°C for the indicated times. Each figure is a representative pattern of 3 independent experiments. (e) Dose-dependent destabilization of fAβ(1–40). The reaction mixtures containing 25 μM fAβ(1–40), 50 mM phosphate buffer, pH 7.5, 100 mM NaCl, and 0, 0.01, 0.1, 1, 10 and 50 μM NDGA (●), Myr (○), Kmp (■), or Cat (□) were incubated at 37°C for 6 h. Points represent means of three independent experiments. In all points, standard errors are within symbols. The average without compounds was regarded as 100%.

Destabilization assay

As shown in Fig. 4(a-d), the fluorescence of ThT was almost unchanged during the incubation of fresh fAβ(1–40) or fAβ(1–42) at 37°C without additional molecules. On the other hand, the ThT fluorescence decreased immediately after addition of polyphenols to the reaction mixture. After incubation of 25 μM fresh fAβ(1–40) with 50 μM Myr for 1 h, many short, sheared fibrils were observed (Fig. 5b). At 6 h, the number of fibrils was reduced markedly, and small amorphous aggregates were occasionally observed (Fig. 5c). Similar morphology was observed when 25 μM fresh fAβ(1–42) were incubated with 50 μM Myr (data not shown). Other polyphenols also destabilized preformed fAβ(1–40) and fAβ(1–42) (data not shown).

After incubation with 50 μM Myr, Mor, Qur or Kmp for 6 h, or 50 μM Cat or epi-Cat for 72 h, fAβ(1–40) and fAβ(1–42) were stained with Congo red to a much lesser degree than fresh fAβ(1–40) and fAβ(1–42). However, they all showed orange-green birefringence under polarized light. This means that a significant amount of intact fAβ(1–40) and fAβ(1–42) still remains in the mixture after the reaction. When the protein concentration of the supernatant after centrifugation at 4°C for 2 h at 1.6×10^4 *g* was measured by the Bradford assay, no proteins were detected in the supernatant in any case. This implies that although polyphenols could destabilize fAβ(1–40) and fAβ(1–42) to

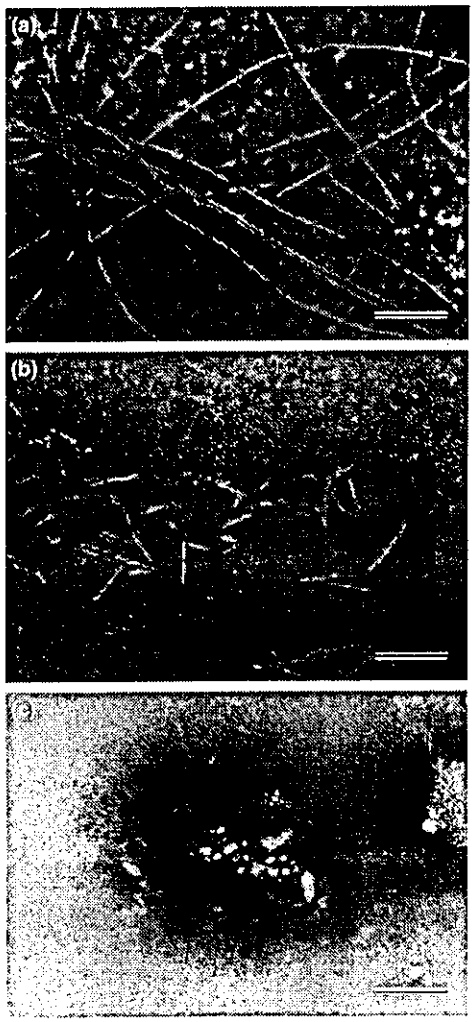

Fig. 5 Electron micrographs of destabilized fAβ(1–40). The reaction mixture containing 25 μM fAβ(1–40), 50 mM phosphate buffer, pH 7.5, 100 mM NaCl, and 50 μM Myr was incubated at 37°C for 0 (a), 1 (b), or 6 h (c). Scale bars indicate a length of 250 nm.

visible aggregates (Fig. 5c), they could not depolymerize fAβ(1–40) and fAβ(1–42) to monomers or oligomers of Aβ(1–40) and Aβ(1–42).

Comparison of the activity of polyphenols

As shown in Figs 1(e), 2(f) and 4(e), NDGA and polyphenols dose-dependently inhibited the formation and extension of fAβs, as well as dose-dependently destabilized pre-formed fAβs. We calculated EC_{50}, the concentrations of NDGA or polyphenols to inhibit the formation or extension of fAβs to 50% of the control value, or the concentrations to destabilize fAβs to 50% of the control value, by the sigmoidal curve fitting of the data as shown in Figs 1(e), 2(f) and 4(e) (Table 1). EC_{50} of NDGA, Myr, Mor, Qur and Kmp to inhibit the formation or extension of fAβs were similar to EC_{50} to destabilize fAβs, respectively. On the other hand, EC_{50} of Cat and epi-Cat to destabilize fAβs were one-order higher than EC_{50} to inhibit the formation or extension of fAβs. All data presented in Table 1 may indicate that the anti-amyloidogenic and fibril-destabilizing activity of the molecules examined in this study may be in the order of: NDGA = Myr = Mor = Qur > Kmp > Cat = epi-Cat.

Cell Cultures and MTT assay

Finally, we examined whether Myr-treated fAβ were toxic to cells. The effects on cell viability were assessed in a simplified model using HEK 293 cell cultures. Cell viability was indirectly measured as a function of the percentage of MTT reduced. Since the dye MTT is known to be converted into a purple formazan by mitochondrial redox activity, MTT reduction assay has been widely used to measure cellular redox activity (Abe and Saito 1998). By measuring the reducing rate of MTT, we recently demonstrated that the cytotoxic effect of Aβ aggregates to HEK 293 cells was similar to that to primary rat hippocampal neurons (Yoshiike *et al.* 2001). As shown in Fig. 6, the cytotoxicity of Myr-treated fAβ(1–40) was significantly lower than that of fAβ(1–40) incubated with 0 (none) or 0.2% DMSO. This suggests that Myr-treated fAβ might be less toxic than intact fAβ. However, the difference in the rate of MTT reduction was not drastic between Myr-treated and intact or DMSO-treated fAβ(1–40). Moreover, since the cultures treated with Myr-treated fAβ(1–40) contained 1 μM Myr, we cannot rule out the possibility that the difference in the rate of MTT reduction may come from the protective effect of Myr itself, for example, through scavenging reactive oxygen species (Choi *et al.* 2001).

Discussion

Recently, our systematic *in vitro* study indicated that the overall activity of the anti-amyloidogenic molecules may be in the order of: NDGA > >RIF = TC > poly(vinylsulfonic acid, sodium salt) = 1,3-propanedisulfonic acid, disodium salt > β-sheet breaker peptide (iAβ5) > nicotine (Ono *et al.* 2002a; Ono *et al.* 2002b). NDGA is smaller than RIF, and has two ortho-dihydroxyphenyl rings symmetrically bound by a short carbohydrate chain. This compact and symmetric structure might be quite suitable for specifically binding to free Aβ and subsequently inhibiting the polymerization of Aβ into fAβ (Ono *et al.* 2002b). Alternatively, this structure might be suitable for a specific binding to fAβ and subsequent destabilization of the β-sheet rich conformation of Aβ molecules in fAβ (Ono *et al.* 2002b). The anti-amyloidogenic and fibril-destabilizing activity of NDGA and polyphenols examined in this study may be in the order of: NDGA = Myr = Mor = Qur > Kmp > Cat = epi-Cat (see Table 1). Some interesting structure-activity relationships of polyphenols could be considered. First, Myr, Mor, Qur and

Table 1 The effective concentrations (EC50)[a] of NDGA and polyphenols for the formation, extension and destabilization of fAβ(1–40) and fAβ(1–42)

Compounds	Formation[b]		Extension[c]		Destabilization[d]	
	fAβ(1–40)	fAβ(1–42)	fAβ(1–40)	fAβ(1–42)	fAβ(1–40)	fAβ(1–42)
NDGA	0.14 μM	0.86 μM	0.23 μM	0.09 μM	1.3 μM	0.87 μM
Myr	0.29	0.40	0.22	0.13	1.8	0.58
Mor	0.24	0.67	0.20	0.14	1.9	0.68
Qur	0.24	0.72	0.25	0.12	2.1	0.73
Kmp	1.7	3.2	0.83	0.45	3.7	2.9
Cat	2.9	5.3	2.4	1.4	28	24
epi-Cat	2.8	5.6	2.4	1.7	23	24

[a]EC_{50} (μM) were defined as the concentrations of NDGA or polyphenols to inhibit the formation or extension of fAbs to 50% of the control value, or the concentrations to destabilize fAbs to 50% of the control value. EC_{50} were calculated by the sigmoidal curve fitting of the data as shown in Figs 1(e), 2(f) and 4(e), using Igor Pro ver.4 (WaveMetrics Inc., Lake Oswego, OR, USA).

[b]The reaction mixtures containing 50 μM Ab(1–40) or 25 μM Ab(1–42), 50 mM phosphate buffer, pH 7.5, 100 mM NaCl, and 0, 0.01, 0.1, 1, 10 and 50 μM NDGA, Myr, Mor, Qur, Kmp, Cat, or epi-Cat were incubated at 37°C for 7 days and 24 h, respectively.

[c]The reaction mixtures containing 10 μg/mL (2.3 μm) sonicated fAb(1–40) or fAb(1–42), 50 μM Ab(1–40) or Ab(1–42), 50 mM phosphate buffer, pH 7.5, 100 mM NaCl, and 0, 0.01, 0.1, 1, 10 and 50 μM NDGA, Myr, Mor, Qur, Kmp, Cat, or epi-Cat were incubated at 37°C for 1 h.

[d]The reaction mixtures containing 25 μM fAb(1–40) or fAb(1–42), 50 mM phosphate buffer, pH 7.5, 100 mM NaCl, and 0, 0.01, 0.1, 1, 10 and 50 μM NDGA, Myr, Mor, Qur, Kmp, Cat, or epi-Cat were incubated at 37°C for 6 h.

Kmp have no chirality and the hydroxyphenyl and benzopyran rings of these molecules are able to be located on the same plane by the rotation of the hydroxyphenyl ring (Fig. 7). On the other hand, Cat and epi-Cat have a chirality and the two rings can not be located on the same plane (Fig. 7). This difference in the three-dimensional structure of polyphenols would greatly affect the anti-amyloidogenic and fibril-destabilizing activity. Secondly, the numbers of hydroxyl groups in Myr, Mor, Qur and Kmp are 6, 5, 5 and 4, respectively (Fig. 7). These numbers would also affect the activity, i.e. the more hydroxyl groups in the molecule, the higher the activity. Tomiyama *et al.* (1994, 1996) suggested that RIF binds to Aβ by hydrophobic interactions between its lipophilic ansa chain and the hydrophobic region of Aβ, thus blocking associations between Aβ molecules leading to fAβ formation. The anti-amyloidogenic and fibril-destabilizing activity of TCs, small-molecule anionic sulfonates or sulfates, melatonin, β-sheet breaker peptides and nicotine may also be related to the propensity to bind to the specific sites of Aβ (Kisilevsky *et al.* 1995; Soto *et al.* 1996; Pappolla *et al.* 1998; Forloni *et al.* 2001; Zeng *et al.* 2001). Interestingly, polyphenols, RIF, melatonin, NDGA and nicotine have all been reported to have antioxidant activity (Goodman *et al.* 1994; Tomiyama *et al.* 1996; Pappolla *et al.* 1998; Linert *et al.* 1999; Bastianetto *et al.* 2000; Choi *et al.* 2001). Thus, it may be reasonable to consider that polyphenols and other organic compounds with antioxidant motifs could bind specifically to Aβ and/or fAβ, inhibit fAβ formation and/or destabilize pre-formed fAβ.

Polyphenols and NDGA did not extend the length of a lag phase in the formation fAβs from Aβs (Fig. 1 and Naiki *et al.* 1998). Moreover, they did not extend the time to proceed to equilibrium in the extension reaction (Fig. 2 and Naiki *et al.* 1998). These results are in sharp contrast to those of apolipoprotein E (apoE), in which apoE extend both the length of a lag phase and the time to proceed to equilibrium in a dose-dependent manner (Naiki *et al.* 1998). Although apoE was suggested to inhibit the formation of fAβs *in vitro*, by making a complex with Aβs, thus eliminating free Aβs from the reaction mixture (Naiki *et al.* 1997, 1998), polyphenols and NDGA would possibly inhibit the formation of fAβs by different mechanisms. As shown in Fig. 2(e), the extension of fAβ(1–40) followed a first-order kinetic model even in the presence of Myr. The net rate of fAβ(1–40) extension is the sum of the rates of polymerization and depolymerization (Naiki and Nakakuki 1996; Hasegawa *et al.* 2002). Thus, one possible explanation for the finding in Fig. 2(e) may be that Myr could bind to the ends of extending fAβ(1–40) and increase the rate of depolymerization by destabilizing the conformation of Aβ(1–40) which has just been incorporated into the fibril ends. Alternatively, Myr would bind to Aβ(1–40) and consequently decrease the rate of polymerization. Further studies are essential to clarify the mechanisms by which polyphenols inhibit fAβ formation *in vitro*.

Recent epidemiological studies have revealed the existence of a negative correlation between moderate red wine drinking and the occurrence of AD (Dartigues and Orgogozo 1993; Dorozynski 1997; Orgogozo *et al.* 1997; Truelsen *et al.* 2002). Our study and several reports on the effects of polyphenols may well explain this correlation. First, Bastianetto *et al.* (2000) showed that major red wine–derived

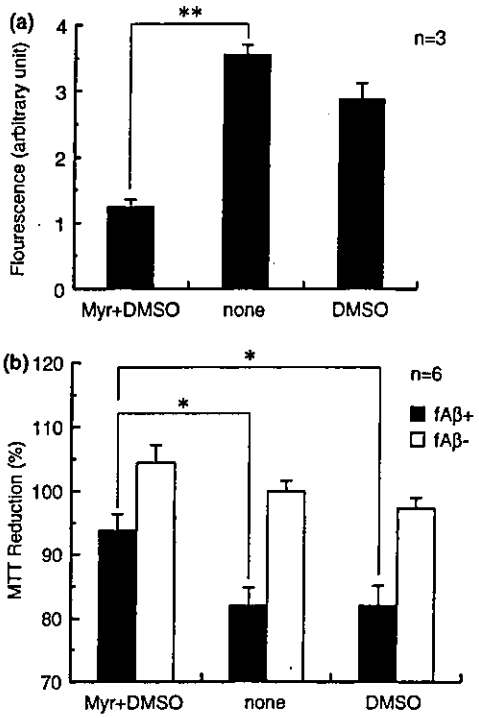

Fig. 6 Cytotoxicity of intact and Myr-treated fAβ(1–40). (a) ThT fluorescence of 10 μM fAβ incubated with 10 μM Myr + 0.2% DMSO (Myr + DMSO), 0 (none) or 0.2% DMSO (DMSO) for 6 h at 37°C was measured right before adding to HEK 293 cell cultures. (b) Cells were treated with a final concentration of 0 (□) or 1 μM (■) Myr-treated (Myr + DMSO), intact (none) or DMSO-treated (DMSO) fAβ1–40 containing 1 μM Myr + 0.02% DMSO, 0 or 0.02% DMSO, respectively, in serum-free DMEM for 2 h and then lysed. Each column represents means + S.E. $^{**}p < 0.001$ (a), $^{*}p < 0.02$ (b) (paired Student's *t*-test).

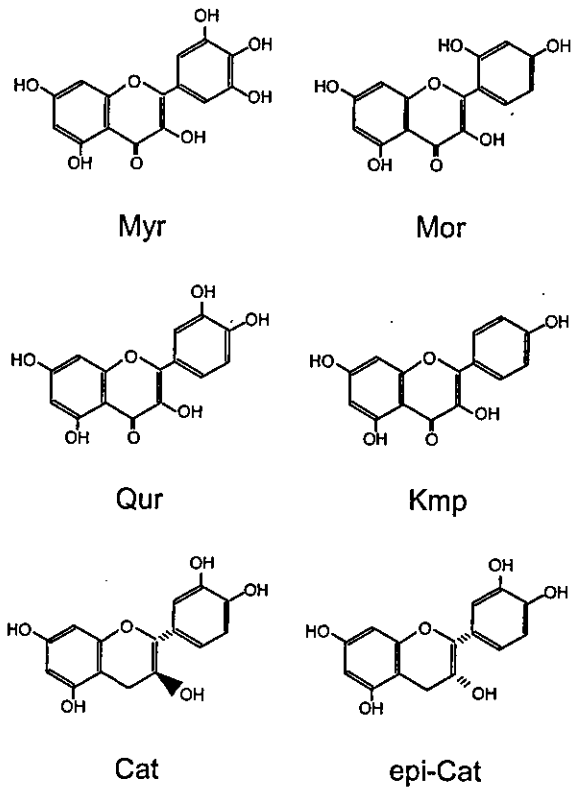

Fig. 7 Structure of Myr, Mor, Qur, Kmp, Cat, and epi-Cat.

polyphenols, such as Qur, resveratrol, and Cat are capable of both protecting and rescuing cultured rat hippocampal cells against nitric oxide-induced toxicity. These effects are probably mediated by antioxidant activities and do not appear to involve purported inhibitory effects on intracellular enzymes such as cyclo-oxygenase, lipoxygenase, nitric oxide synthase and, with the exception of Qur, protein kinase C. Similarly, Choi *et al.* (2001) reported that the green tea polyphenol (–)-epigallocatechin gallate attenuates Aβ-induced neurotoxicity through scavenging reactive oxygen species in cultured hippocampal neurons. Virgili and Contestabile (2000) showed that chronic administration of resveratrol to young-adult rats significantly protects from the damage caused by systemic injection of the excitotoxin kainic acid, in the olfactory cortex and the hippocampus. Similarly, Inanami *et al.* (1998) reported that oral administration of Cat dose-dependently protects against ischemia-reperfusion-induced cell death of hippocampal CA1 in the gerbil. They also showed that superoxide scavenging activities of the brains obtained from Cat-treated gerbils were significantly higher than those of Cat-untreated animals, suggesting that orally administered Cat was absorbed, passed through the blood–brain barrier (BBB) and protected against neuronal death due to its antioxidant activities. Suganuma *et al.* (1998) also demonstrated that the green tea polyphenol (–)-epigallocatechin gallate administered *per os* could pass BBB and reach brain parenchyma in mice. It is therefore conceivable that moderate, daily consumption of red wine could provide sufficient amount of active phenolic compounds to the brain to offer neuroprotection. Finally, as shown in this paper, polyphenols dose-dependently inhibit fAβ formation from fresh Aβ, as well as destabilize preformed fAβ *in vitro*. Moreover, cell culture experiments with HEK 293 cells suggested that fAβ treated by Myr might be less toxic than intact fAβ. Thus, it may be reasonable to speculate that red wine-derived polyphenols could prevent the development of AD, not only through scavenging reactive oxygen species, but also through directly inhibiting the deposition of fAβ in the brain. Although the exact mechanisms of anti-amyloidogenic and fibril-destabilizing activity of polyphenols are unclear, polyphenols could be a key molecule for the development of therapeutics for AD and other human amyloidoses.

Acknowledgements

The authors thank Dr S. Okino and Dr K. Iwasa (Kanazawa University) for co-operation in the experiments, and Mrs H. Okada and Mr N. Takimoto (Fukui Medical University) for excellent technical assistance.

This work was supported in part by a Grant-in-Aid for Scientific Research from the Ministry of Education, Culture, Sports, Science and Technology, Japan (M.Y and H.N), a grant to the Amyloidosis Research Committee from the Ministry of Health, Labour, and Welfare, Japan (M.Y and H.N), and a Grant-in-Aid for Scientific Research on Priority Areas (C) -Advanced Brain Science Project- from the Ministry of Education, Culture, Sports, Science and Technology, Japan (H.N).

References

Abe K. and Saito H. (1998) Amyloid beta protein inhibits cellular MTT reduction not by suppression of mitochondrial succinate dehydrogenase but by acceleration of MTT formazan exocytosis in cultured rat cortical astrocytes. *Neurosci. Res.* **31**, 295–305.

Bastianetto S., Zheng W. H. and Quirion R. (2000) Neuroprotective abilities of resveratrol and other red wine constituents against nitric oxide-related toxicity in cultured hippocampal neurons. *Br. J. Pharmacol.* **131**, 711–720.

Bradford M. M. (1976) A rapid and sensitive method for the quantitation of microgram quantities of protein utilizing the principle of protein-dye binding. *Anal. Biochem.* **72**, 248–254.

Celotti E., Ferrarini R., Zironi R. and Conte L. S. (1996) Resveratrol content of some wines obtained from dried Valpolicella grapes: Recioto and Amarone. *J. Chromato.* **730**, 47–52.

Cherny R. A., Atwood C. S., Xilinas M. E., Gray D. N., Jones W. D., McLean C. A., Barnham K. J., Volitakis I., Fraser F. W., Kim Y.-S., *et al.* (2001) Treatment with a copper-zinc chelator markedly and rapidly inhibits beta-amyloid accumulation in Alzheimer's disease transgenic mice. *Neuron* **30**, 665–676.

Choi Y. T., Jung C. H., Lee S. R., Bae J. H., Baek W. K., Suh M. H., Park J., Park C. W. and Suh S. I. (2001) The green tea polyphenol (-)-epigallocatechin gallate attenuates beta-amyloid-induced neurotoxicity in cultured hippocampal neurons. *Life Sci.* **70**, 603–614.

Dartigues J. F. and Orgogozo J. M. (1993) Wine consumption in the elderly. *Ann. Intern. Med.* **118**, 317–318.

Doody R. S., Stevens J. C., Beck C., Dubinsky R. M., Kaye J. A., Gwyther L., Mohs R. C., Thal L. J., Whitehouse P. J., DeKosky S. T. and Cummings J. L. (2001) Practice parameter: management of dementia (an evidence-based review). Report of the Quality Standards Subcommittee of the American Academy of Neurology. *Neurology* **56**, 1154–1166.

Dorozynski A. (1997) Wine may prevent dementia. *Br. Med. J.* **314**, 997.

Forloni G., Colombo L., Girola L., Tagliavini F. and Salmona M. (2001) Anti-amyloidogenic activity of tetracyclines: studies *in vitro*. *FEBS Lett.* **487**, 404–407.

Goldberg D. M., Tsang E., Karumanchiri A., Diamandis E. P., Soleas G. and Ng E. (1996) Method to assay the concentrations of phenolic constituents of biological interest in wines. *Anal. Chem.* **68**, 1688–1694.

van Golde P. H., Sloots L. M., Vermeulen W. P., Wielders J. P., Hart H. C., Bouma B. N. and van de Wiel A. (1999) The role of alcohol in the anti low density lipoprotein oxidation activity of red wine. *Atherosclerosis* **147**, 365–370.

Goodman Y., Steiner M. R., Steiner S. M. and Mattson M. P. (1994) Nordihydroguaiaretic acid protects hippocampal neurons against amyloid beta-peptide toxicity, and attenuates free radical and calcium accumulation. *Brain Res.* **654**, 171–176.

Hasegawa K., Yamaguchi I., Omata S., Gejyo F. and Naiki H. (1999) Interaction between A beta (1–42) and A beta (1–40) in Alzheimer's beta-amyloid fibril formation *in vitro*. *Biochemistry* **38**, 15514–15521.

Hasegawa K., Ono K., Yamada M. and Naiki H. (2002) Kinetic modeling and determination of reaction constants of Alzheimer's β-amyloid fibril extension and dissociation using surface plasmon resonance. *Biochemistry* **41**, 13489–13498.

Hertog M. G. L., Hollman P. C. H. and van de Putte B. (1993) Content of potentially anticarcinogenic flavonoids of tea infusions, wines, and fruit juices. *J. Agric. Food Chem.* **41**, 1242–1246.

Inanami O., Watanabe Y., Syuto B., Nakano M., Tsuji M. and Kuwabara M. (1998) Oral administration of (-) catechin protects against ischemia-reperfusion-induced neuronal death in the gerbil. *Free Radic. Res.* **29**, 359–365.

Jarrett J. T. and Lansbury P. T. Jr (1993) Seeding 'one-dimensional crystallization' of amyloid: a pathogenic mechanism in Alzheimer's disease and scrapie? *Cell* **73**, 1055–1058.

Kisilevsky R., Lemieux L. J., Fraser P. E., Kong X., Hultin P. G. and Szarek W. A. (1995) Arresting amyloidosis in vivo using small-molecule anionic sulphonates or sulphates: implications for Alzheimer's disease. *Nat. Med.* **1**, 143–148.

Levites Y., Weinreb O., Maor G., Youdim M. B. and Mandel S. (2001) Green tea polyphenol (-)-epigallocatechin-3-gallate prevents N-methyl-4-phenyl-1,2,3,6-tetrahydropyridine-induced dopaminergic neurodegeneration. *J. Neurochem.* **78**, 1073–1082.

Linert W., Bridge M. H., Huber M., Bjugstad K. B., Grossman S. and Arendash G. W. (1999) *In vitro* and *in vivo* studies investigating possible antioxidant actions of nicotine: relevance to Parkinson's and Alzheimer's diseases. *Biochim. Biophys. Acta* **1454**, 143–152.

Lomakin A., Teplow D. B., Kirschner D. A. and Benedek G. B. (1997) Kinetic theory of fibrillogenesis of amyloid beta-protein. *Proc. Natl Acad. Sci. U.S.A.* **94**, 7942–7947.

Naiki H. and Gejyo F. (1999) Kinetic analysis of amyloid fibril formation. *Meth. Enzymol.* **309**, 305–318.

Naiki H. and Nakakuki K. (1996) First-order kinetic model of Alzheimer's beta-amyloid fibril extension *in vitro*. *Laboratory Invest.* **74**, 374–383.

Naiki H., Gejyo F. and Nakakuki K. (1997) Concentration-dependent inhibitory effects of apolipoprotein E on Alzheimer's beta-amyloid fibril formation *in vitro*. *Biochemistry* **36**, 6243–6250.

Naiki H., Hasegawa K., Yamaguchi I., Nakamura H., Gejyo F. and Nakakuki K. (1998) Apolipoprotein E and antioxidants have different mechanisms of inhibiting Alzheimer's beta-amyloid fibril formation *in vitro*. *Biochemistry* **37**, 17882–17889.

Ono K., Hasegawa K., Yamada M. and Naiki H. (2002a) Nicotine breaks down preformed Alzheimer's beta-amyloid fibrils *in vitro*. *Biol. Psychiatry* **52**, 880–886.

Ono K., Hasegawa K., Yoshiike Y., Takashima A., Yamada M. and Naiki H. (2002b) Nordihydroguaiaretic acid potently breaks down preformed Alzheimer's beta-amyloid fibrils *in vitro*. *J. Neurochem.* **81**, 434–440.

Orgogozo J. M., Dartigues J. F., Lafont S., Letenneur L., Commenges D., Salamon R., Renaud S. and Breteler M. B. (1997) Wine consumption and dementia in the elderly: a prospective community study in the Bordeaux area. *Rev. Neurol. (Paris)* **153**, 185–192.

Pappolla M., Bozner P., Soto C., Shao H., Robakis N. K., Zagorski M., Frangione B. and Ghiso J. (1998) Inhibition of Alzheimer beta-fibrillogenesis by melatonin. *J. Biol. Chem.* **273**, 7185–7188.

Renaud S. and de Lorgeril M. (1992) Wine, alcohol, platelets, and the French paradox for coronary heart disease. *Lancet* **20**, 1523–1526.

Sato M., Suzuki Y., Okuda T. and Yokotsuka K. (1997) Contents of resveratrol, piceid, and their isomers in commercially available wines made from grapes cultivated in Japan. *Biosci. Biotech. Biochem.* **61**, 1800–1805.

Schenk D., Barbour R., Dunn W., Gordon G., Grajeda H., Guido T., Hu K., Huang J., Johnson-Wood K., Khan K. *et al.* (1999) Immunization with amyloid-beta attenuates Alzheimer-disease-like pathology in the PDAPP mouse. *Nature* **400**, 173–177.

Selkoe D. J. (2001) Alzheimer's disease: genes, proteins, and therapy. *Physiol. Rev.* **81**, 741–766.

Shutenko Z., Henry Y., Pinard E., Seylaz J., Potier P., Berthet F., Girard P. and Sercombe R. (1999) Influence of the antioxidant quercetin in vivo on the level of nitric oxide determined by electron paramagnetic resonance in rat brain during global ischemia and reperfusion. *Biochem. Pharmacol.* **57**, 199–208.

Soleas G. J., Diamandis E. P. and Goldberg D. M. (1997) Resveratrol: a molecule whose time has come? and gone? *Clin. Biochem.* **30**, 91–113.

Soto C., Kindy M. S., Baumann M. and Frangione B. (1996) Inhibition of Alzheimer's amyloidosis by peptides that prevent beta-sheet conformation. *Biochem. Biophys. Res. Commun.* **226**, 672–680.

Suganuma M., Okabe S., Oniyama M., Tada Y., Ito H. and Fujiki H. (1998) Wide distribution of [3H] (-)-epigallocatechin gallate, a cancer preventive tea polyphenol, in mouse tissue. *Carcinogenesis* **19**, 1771–1776.

Tomiyama T., Asano S., Suwa Y., Morita T., Kataoka K., Mori H. and Endo N. (1994) Rifampicin prevents the aggregation and neurotoxicity of amyloid beta protein *in vitro*. *Biochem. Biophys. Res. Commun.* **204**, 76–83.

Tomiyama T., Shoji A., Kataoka K., Suwa Y., Asano S., Kaneko H. and Endo N. (1996) Inhibition of amyloid beta protein aggregation and neurotoxicity by rifampicin. Its possible function as a hydroxyl radical scavenger. *J. Biol. Chem.* **271**, 6839–6844.

Truelsen T., Thudium D. and Gronbaek M. (2002) Amount and type of alcohol and risk of dementia: the Copenhagen City Heart Study. *Neurology* **59**, 1313–1319.

Virgili M. and Contestabile A. (2000) Partial neuroprotection of in vivo excitotoxic brain damage by chronic administration of the red wine antioxidant agent, trans-resveratrol in rats. *Neurosci. Lett.* **281**, 123–126.

Yoshiike Y., Tanemura K., Murayama O., Akagi T., Murayama M., Sato S., Sun X., Tanaka N. and Takashima A. (2001) New insights on how metals disrupt amyloid beta-aggregation and their effects on amyloid-beta cytotoxicity. *J. Biol. Chem.* **276**, 32293–32299.

Zeng H., Zhang Y., Peng L.-J., Shao H., Menon N. K., Yang J., Salomon A. R., Freidland R. P. and Zagorski M. G. (2001) Nicotine and amyloid formation. *Biol. Psychiatry* **49**, 248–257.

別紙一覧(平成 14 年度ー16 年度)

発表者	論文名	発表誌	巻号	ページ	出版年
Takashima A	The role of GSK-3ß in the formation of neurofibrillary tangles	Psychogeriatrics	4	17-22	2004
Shigetsugu H, Matsumoto M, Kamura T, Murayama M, Chui D-H, Planel E, Takahashi R, Nakayama K-I, and Takashima A	U-box protein carboxyl terminus of Hsc7-interacting protein (CHIP) mediates poly-ubiquitylation preferentially on four-repeat Tau and is involved in neurodegeneration of tauopathy	J.Neurochem	91	299-307	2004
Planel E, Miyasaka T, Launey T, Chui D-H, Tanemura K, Sato S, Murayama O, Ishiguro K, Tatebayashi Y, Takashima A	Alterations in glucose metabolism induce hypothermia leading to tau hyperphosphorylation: mechanism and implications for Alzheimer's disease	J Neurosci	24	2401-2411	2004
Hashimoto Y, Tsukamoto E, Niikura T, Yamagishi Y, Ishizaka M, Aiso S, Takashima A, Nishimoto I	Amino- and carboxyl-terminal mutants of presenilin 1 cause neuronal cell death through distinct toxic mechanisms: Study of 27 different presenilin 1 mutants	J Neurosci Res	75 (3)	417-428	2004
Dou F, Netzer WJ, Tanemura K, Li F, Hartl FU, Takashima A, Gouras GK, Greengard P, Xu H.	Chaperones increase association of tau protein with microtubules	Proc Natl Acad Sci U S A	Jan 21;100(2)	721-6	2003
Kwok JBJ, Halliday GM, Brrok WS, Dolios G., Laudon H., Murayama O., Hallupp M., Badenhop RF, Vick J., Eang R., Naslund J., Takashima, A., Gandy SE, Schofield PR.	Presenilin-1 mutation (Leu271 Val) results in altered exonic splicing and Alzheimer's disease with non-cored plaques and neuritic dystrophy	J Biol Chem	278(9)	6748-6754	2003

Yuji Yoshiike, De-Hua Chui, Takumi Akagi, Nobuo Tanaka, and Akihiko Takashima	Specific compositions of amyloid-ß peptides as the determinant of toxic ß-aggregation	The Journal of Biological Chemitry	278;26	23648-23655	2003
Kenjiro Ono, Yuji Yosiike, Akihiko Takashima, Kazuhiro Hasegawa, Hironobu Naiki, and Masahito Yamada	Potent anti-amyloidogenic and fibril-destabilizing effects of polyphenols *in vitro*: implications for the prevention and therapeutics of Alzheimer's disease	The Journal of Neurochemistry	87	172-181	2003
Philippe Marambaud, Paul H. Wen, Anindita Dutt, Junichi Shioi, Akihiko Takashima, Robert Siman, and Nikolaos K. Robakis	A CBP binding transcriptional repressor produced by the PS1/e-cleavage of N-cadherin is inhibited by PS1 FAD mutants	Cell	114	635-645	2003
Planel E,Sun, X, Takashima A	Role of GSK -3ß in Alzheimer's disease pathology	Drug Dev. Res	56	491-510	2002
Sato, S, Tatebayashi, Y., Akagi, T., Chui, D-H, Murayama, M., Miyasaka, T., Planel, E., Tanemura, K., Sun, X, Hashikawa, T., Yoshioka, K., Ishiguro, K., Takashima, A	Aberrant tau phosphorylation by GSK-3ß and JNK-3 induces oligomeric tau fibrils in COS-7 cells	J. biol Chem	277	42060-42065	2002
Tatebayashi, Y. Miyasaka, T, Chui, D-H, Akagi, T., Mishima, K., Iwasaki, K., Fujiwara, M., Tanemura, K., Murayama, M., Ishiguro, K., Planel, E., Sato, S., Hashikawa, T., Takashima, A	Tau filament formation and associative memory deficit in aged mice expressing mutant (R406W) human tau	Proc Natl Acad Sci U S A	99	13896-13901	2002
Ono K, Hasegawa K, Yoshiike Y, Takashima A, Yamada M, Naiki H	Nordihydroguaiaretic acid potently breaks down pre-formed Alzheimer's beta-amyloid fibrils in vitro	J Neurochem	81(3)	434-40	2002

Xia X, Wang P, Sun X, Soriano S, Shum WK, Yamaguchi H, Trumbauer ME, Takashima A, Koo EH, Zheng H	The aspartate-257 of presenilin 1 is indispensable for mouse development and production of {beta}-amyloid peptides through {beta}-catenin-independent mechanisms	Proc Natl Acad Sci U S A	99	8760-8765	2002
Tanemura, K., Akagi T., Murayama, M., Hashikawa, T., Tominaga T., Ichikawa, M., Yamaguchi, H., and Takashima, A	Neurodegeneration with tau accumulation in a transgenic mouse expressing V337M human tau	J. Neurosci	22	133-141	2002
X. Sun, S. Sato, O. Murayama, M. Murayama, J.-M. Park, H. Yamaguchi, and Takashima A	Lithium inhibits amyloid secretion in COS7 cells transfected with amyloid precursor protein C100	Neurosci. lett	15	61-64	2002
Sun, X, Cole, GM, Chu, T., Xia, W., Galasko, D., Yamaguchi, H., Frautschy SA., Takashiima A	Intracellular Aß is increased by okadaic acid exposure in the transfected neuronal and non-neuronal cell lines	Neurobiol. of Aging	23	195-203	2002

Available online at www.sciencedirect.com
SCIENCE DIRECT
Neuroscience Letters 374 (2005) 47–52
Neuroscience Letters
www.elsevier.com/locate/neulet

Possible involvement of the expression and phosphorylation of N-Myc in the induction of HMGA1a by hypoxia in the human neuroblastoma cell line

Takeshi Yanagita[a,1], Takayuki Manabe[a,*,1], Hiroaki Okuda[a], Shinsuke Matsuzaki[a], Yoshio Bando[b], Taiichi Katayama[a,c], Masaya Tohyama[a]

[a] *Department of Anatomy and Neuroscience, Graduate School of Medicine, Osaka University, 2-2 Yamadaoka, Suita, Osaka, Japan*
[b] *Department of Anatomy, Asahikawa Medical College, Asahikawa, 078-8510 Hokkaido, Japan*
[c] *Innovation Plaza Osaka, Izumisano, Osaka, Japan*

Received 12 August 2004; received in revised form 8 October 2004; accepted 9 October 2004

Abstract

Increased expression of N-Myc and expression of the high mobility group protein A1a (HMGA1a) were observed in the nuclei of SK-N-SH cells following exposure to hypoxia. These observations were accompanied by the appearance of additional high molecular weight bands, which were eliminated by pretreatment with alkaline phosphatase. Immunoprecipitation showed phosphorylation of serine, threonine and tyrosine residues of N-Myc in the nucleus. These results suggest that hypoxia-induced signals in SK-N-SH cells lead to persistent expression of HMGA1a, which may induce expression of the transcription factor N-Myc, and that phosphorylation at serine, threonine and tyrosine residues of N-Myc occurs at an early stage after stimulation. Such signal consolidation processes could play a role in neuronal survival after hypoxia in neurons.

Keywords: Hypoxia; HMGA1a; Myc family members; Phosphorylation; Neuroblastoma

Alzheimer's disease (AD) is a neurodegenerative disorder that has several pathological characteristics: severe neuron loss, glial proliferation, extracellular deposition of senile plaques composed of beta-amyloid, and deposition of intracellular neurofibrillary tangles [39]. Recently, we discovered that an alternative splice variant of the *presenilin*-2 (*PS2*) gene that lacks exon 5 (PS2V) is significantly expressed in the brains of sporadic AD patients, compared with those of controls [35]. PS2V encodes aberrant proteins that form intracellular inclusion bodies (PS2V bodies) [20], and these are present in pyramidal cells of the cerebral cortex and the hippocampus in 100% of sporadic AD brains [36]. Furthermore, cell lines that express PS2V become fragile in response to various endoplasmic reticulum (ER) stresses [35,36], leading to changes in the conformation of tau proteins [25].

The expression of PS2V observed in sporadic AD is mimicked in hypoxia-exposed human neuroblastoma SK-N-SH cells [35,36]. PS2V is induced by the action of the high mobility group protein A1a (HMGA1a), which directly binds to specific sequences on PS2 pre-mRNA in SK-N-SH cells following hypoxic stimulation [19]. Furthermore, increased expression of the HMGA1a protein has been observed in the hippocampus of sporadic AD brains and nuclear extracts from hypoxia-exposed SK-N-SH cells, compared with those from controls cells under normoxia [19]. The protein has been observed to accumulate in nuclear speckles, along with the endogenous splicing factor SC35 [19].

Abbreviations: HMGA1a, high molecular group protein A1a; PS, phosphoserine; PT, phosphothreonine; PY, phosphotyrosine

* Corresponding author. Present address: Department of Anatomy, Nara Medical University, 840 Shijyo-cho, Kashihara City, 634-8521 Nara, Japan. Tel.: +81 744 29 8825; fax: +81 744 29 8825.
E-mail address: manabe@naramed-u.ac.jp (T. Manabe).
[1] These authors contributed equally to this work.

0304-3940/$ – see front matter © 2004 Elsevier Ireland Ltd. All rights reserved.
doi:10.1016/j.neulet.2004.10.039

Members of the HMGA protein family participate in many cellular processes, including regulation of inducible gene transcription, integration of retroviruses into chromosomes, and metastatic progression of cancer cells [31]. HMGA proteins contain three copies of a conserved DNA-binding peptide motif called the 'AT-hook', which preferentially binds to the AT-rich DNA minor groove and interacts in vivo with a large number of other proteins, many of which are transcription factors.

A previous study has shown that HMGA1a is a direct c-Myc-targeted gene involved in neoplastic transformation in Burkitt's lymphoma [43]. The Myc family proteins, N-Myc and c-Myc, are implicated in the regulation of cell proliferation, differentiation and apoptosis [5,13,28,29]. It is likely that c-Myc expression is differentially activated in various paradigms of neuronal cell death in vivo and in vitro [1,23,24], and it has been suggested that N-Myc function depends on cell type and developmental stage, as well as on the external environment [3,37,41]. On the other hand, previous reports have demonstrated that N-Myc, c-Myc and phosphorylated c-Myc are present in the AD brain and in brains affected by other neurodegenerative diseases [7,8]. Furthermore, more potent expression of c-Myc protein and c-*myc* mRNA have been observed in ischemic rodent brains [23,24], and previous reports have demonstrated that hypoxia promotes apoptosis of human neuroblastoma cell lines through enhanced N-Myc expression [32].

It is known that the functions and DNA-binding activities of Myc family proteins are regulated by phosphorylation [9–12,14–17,26,27,33,34,40,42]. Furthermore, Myc function requires heterodimerization of the Myc and Max basic/helix–loop–helix/leucine zipper (bHLHZ) domains prior to sequence-specific DNA binding. Myc–Max heterodimers recognize a core hexanucleotide element (5′-CACGTG-3′), termed the Enhancer box or E box [4,30], and activate transcription at promoters containing such E boxes [2,6].

The role of Myc family proteins in neurodegenerative disorders is poorly understood. In this manuscript, we propose a hypothesis involving a novel neurotoxic pathway that includes expression and phosphorylation of N-Myc by hypoxic induction of HMGA1a, leading to neuronal cell death via induction of PS2V expression.

In brief, human neuroblastoma SK-N-SH and human HEK293T cells were cultured in α-minimal essential and Dulbecco's modified Eagle's medium supplemented with fetal calf serum, respectively. When cells achieved confluence in 175 cm^2 culture plate, the medium was exchanged with serum-free medium. After 4 h, cultures were exposed to hypoxia for 0–21 h using an incubator equipped with low oxygen tension (8 Torr within 3–5 h after cultures were transferred to the hypoxia chamber).

The nuclear fraction was prepared as previously described [38] with minor modifications [18,44,45]. In brief, samples were homogenized in 50 volumes of 10 mM HEPES-NaOH buffer (pH 7.9) containing 10 mM KCl, 1 mM EDTA, 1 mM EGTA, 5 mM dithiothreitol, 10 mM NaF, 10 mM sodium β-glycerophosphate (NaGP), 10 mM sodium pyrophosphate 1 mM sodium orthovanadate (OV), and 1 μg/ml of PMSF at 2 °C. Following the addition of 10% Nonidet P-40 to make a final concentration of 0.6%, homogenates were centrifuged at 15,000 × *g* for 5 min to obtain nuclear fractions. Pellets thus obtained were suspended in 5–10 volumes of 20 mM Tris–HCl buffer (pH 7.5) containing 1 mM EDTA, 1 mM EGTA, 10 mM NaF, 10 mM NaGP, 10 mM sodium pyrophosphate 1 mM OV and 1 μg/ml of PMSF. Immunoblotting was performed as previously described [21,22].

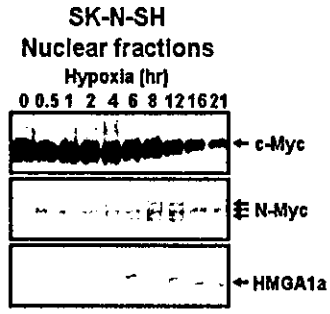

Fig. 1. Effects of hypoxia stimulation on expression of Myc family proteins in human neuroblastoma SK-N-SH cells. Nuclear fractions from SK-N-SH cells were prepared after 0–21 h hypoxia stimulation, followed by immunoblotting assay using anti-c-Myc (top), anti-N-Myc (middle) and anti-HMGA1a (bottom) antibodies.

Nuclear fractions from SK-N-SH cells were obtained after hypoxic stimulation for 0–21 h. These fractions were then subjected to SDS–PAGE and immunoblotting analysis. No significant increase in immunoreactivity was found using an antibody against c-Myc protein (see the corresponding molecular weight position indicated by the black arrow in Fig. 3a and the upper panel of Fig. 1), but PS2V was induced under hypoxic conditions (Fig. 3b) [19,35,36]. On the other hand, exposure to hypoxia for 6 h significantly potentiated N-Myc expression in SK-N-SH cells, with about a 1.5-fold potentiation 8–16 h after exposure to hypoxia (Fig. 3a and the middle panel of Fig. 1b). This potentiation persisted for at least 21 h, after which no further measurements were made (Fig. 3a and the middle panel of Fig. 1b). In contrast, hypoxia did not significantly potentiate HMGA1a expression in SK-N-SH cells following 8 h or less of hypoxic stimulation (Fig. 3a and the middle panel of Fig. 1c). However, increased hypoxic exposure for 8–21 h did lead to stimulation-time dependent expression of HMGA1a in the nuclei of SK-N-SH cells, as observed for N-Myc induction (Fig. 3a and the middle panel of Fig. 1c).

Exposure to hypoxia for 0.5–21 h, under which conditions PS2V expression was not induced, did not significantly alter N-Myc expression in HEK-293T cells (Fig. 3a and the middle panel of Fig. 2). In contrast, hypoxia significantly potentiated c-Myc expression in HEK-293T cells following 1–12 h of hypoxic stimulation, with a decline to control levels thereafter (Fig. 3a and the upper panel of Fig. 2). On the other hand,

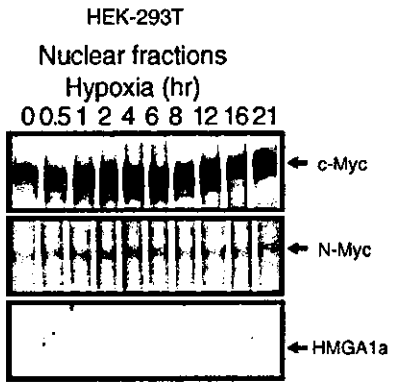

Fig. 2. Effects of hypoxia stimulation on expression of Myc family proteins in HEK-293T cells. Nuclear fractions from HEK-293T cells were prepared after 0–21 h hypoxia stimulation, followed by immunoblotting assay using anti-c-Myc (top), anti-N-Myc (middle) or anti-HMGA1a (bottom) antibodies.

no significant hypoxia-induced expression of HMGA1a was seen in the nuclear fraction from HEK-293T cells (Fig. 3a and the lower panel of Fig. 2). Hence, the hypoxia-induced expression patterns of these proteins differed between SK-N-SH cells and HEK-293T cells (Fig. 3a).

As shown in Fig. 1, hypoxia in SK-N-SH cells potentiated not only N-Myc expression but also additional bands of a higher molecular weight than normal N-Myc (Fig. 4a). Therefore, we investigated whether the high mobility bands produced by hypoxia were due to phosphorylation of the N-Myc protein. Pretreatment with alkaline phosphatase (AP) eliminated the high mobility bands in the nuclear fraction from hypoxia-exposed SK-N-SH cells (Fig. 4b, highest arrow), presumably due to dephosphorylation, and resulted in a large increase in the immunoreactivity of the lowest molecular weight band (Fig. 4b, lowest arrow). Then, the binding activity of N-Myc to its target region in HMGA1a promoter was analyzed by gel retardation shift asaay using the nuclear extracts from normoxia (lane 1), hypoxia (8 h, lane 2) and hypoxia (8 h) + pretreatment with AP (lane 3) (Fig. 4c). The increased binding activity by hypoxia (lane 2) was disappeared in the AP-pretreated nucrear extracts (Fig. 4c, lane 3). Therefore, these results suggest that the reinforced N-Myc expression and phosphorylation by hypoxia lead to activation of HMGA1a transcription. Given these results, nuclear fractions were prepared from SK-N-SH cells after 8 h of hypoxic stimulation, followed by immunoprecipitation with the anti-N-Myc antibody, SDS–PAGE and immunoblotting using an-

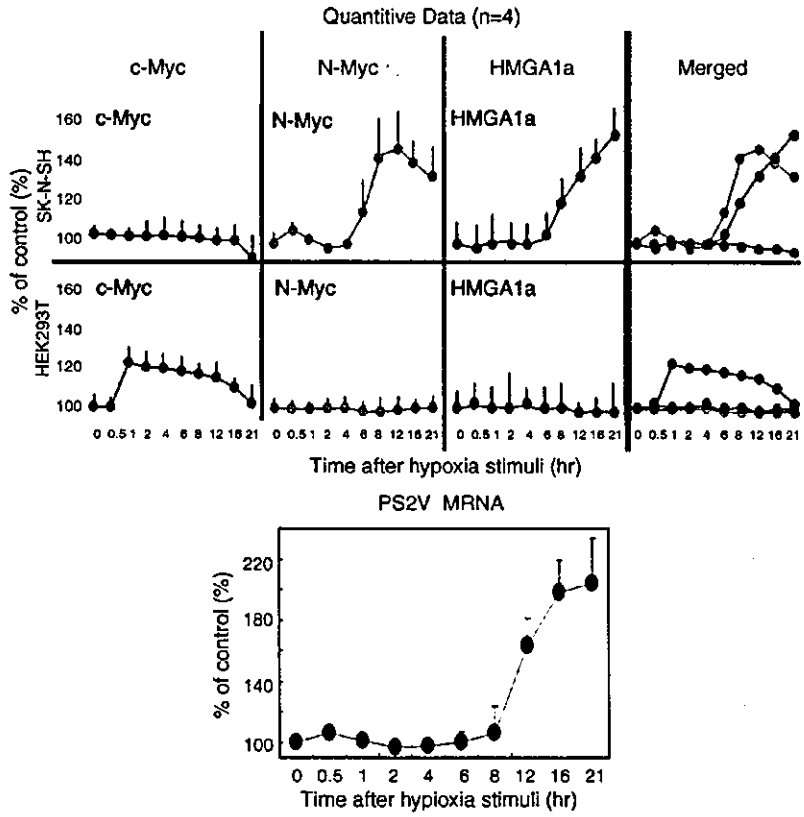

Fig. 3. (a) Quantitative data of Figs. 1 and 2. Data are mean ± S.E. ($n = 3$). c-Myc, N-Myc, HMGA1a and all-merged data of Fig. 1 (upper) and Fig. 2 (lower) were shown. (b) Effects of hypoxia stimulation on expression of PS2V mRNA in SK-N-SH cells. Total RNA from SK-N-SH cells were prepared after 0–21 h hypoxia stimulation, followed by RT-PCR assay as described previously [18,36]. Quantitative data was shown. Data are mean ± S.E. ($n = 3$).

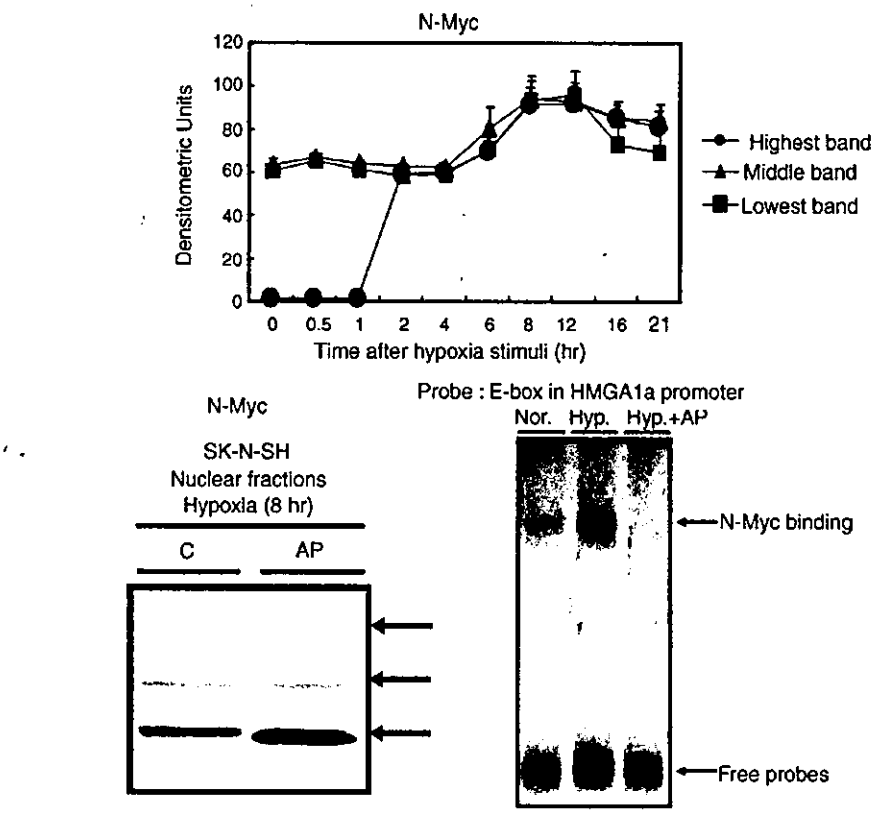

Fig. 4. Effects of alkaline phosphatase on appearance of immunoreactive N-Myc proteins by hypoxia in nuclear fractions from SK-N-SH cells. (a) Individual quantitative data of three different bands in N-Myc were shown. Data are mean ± S.E. ($n = 3$). (b) SK-N-SH cells were stimulated for 8 h under hypoxia, followed by preparation of nuclear fractions. Samples were treated with or without alkaline phosphatase and a subsequent immunoblotting assay using an anti-N-Myc antibody. (c) Effects of alkaline phosphatase (AP) treatment on N-Myc binding with the E-box of HMGA1a promoter in each nuclear extract. Cells were incubated under the normoxic or hypoxic condition for 8 h, followed by collection and preparation of nucrear extracts. AP-treated or untreated samples were subjected to gel retardation electrophoresis and subsequently autoradiography.

tibodies against phosphotyrosine (PY, Fig. 5a), phosphothreonine (PT, Fig. 5b) and phosphoserine (PS, Fig. 5c) to detect possible phosphorylation of N-Myc. Three immunoreactive bands against anti-PS antibody were detected in immunoprecipitates that co-precipitated with anti-N-Myc antibody

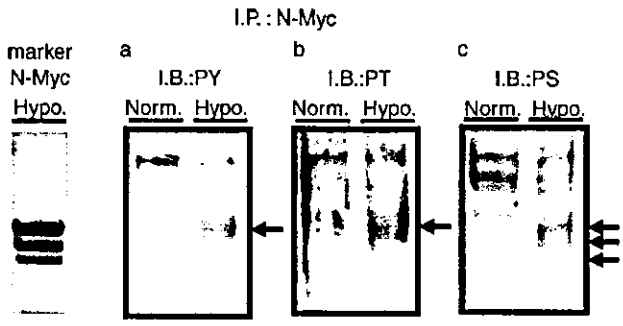

Fig. 5. Effects of hypoxia on phosphorylation of immunoreactive N-Myc protein in nuclear fractions of SK-N-SH cells. Samples were immunoprecipitated with an anti-N-Myc antibody following an immunoblotting assay using anti-phosphotyrosine (a; PY), anti-phosphothreonine (b; PT) or anti-phosphoserine (c; PS) antibodies.

(Fig. 5c, left panel) after hypoxic stimulation for 8 h (Fig. 5c). Strong immunoreactivity to antibodies against PY (Fig. 5a) and PT (Fig. 5b) was also observed in immunoprecipitates obtained after hypoxic stimulation for 8 h.

The primary importance of the present findings is that hypoxic stimulation led to differential expression of particular Myc family proteins in nuclear fractions of cell lines, and that this expression occurred in a manner dependent on the hypoxia exposure time. Our previous data showed that exposure to hypoxia for 10–18 h does not induce any significant changes in the expression of HMGA1a protein, HMGA1a mRNA, and PS2V mRNA in non-neuronal cell lines, including HEK293T and HeLa cells, compared with normoxia [19]. The findings in the present study clearly demonstrate that exposure to 0.5–21 h of hypoxia does not induce N-Myc and HMGA1a expression in nuclear fractions from 293T cells (Fig. 2, lower and middle panels). However, transient induction of c-Myc was observed in nuclear fractions from 293T cells (Fig. 2, upper panel). These data suggest that HMGA1a induction by hypoxia does not depend on c-Myc expression, although it has been shown that the HMGA1a gene is directly targeted by c-Myc under other conditions [43].

There are two possible explanations for this inconsistency. One involves participation of the N-Myc protein. Considering that hypoxic stimulation of SK-N-SH cells was performed under PS2V-inducible conditions (Fig. 3b) [19,35,36] (i.e., HMGA1a-inducible conditions [19]), the expression of N-Myc and HMGA1a proteins is in good temporal agreement. That is, the appearance of HMGA1a and PS2V may follow that of N-Myc and HMGA1a, respectively (Fig. 2, lower and middle panels; Fig. 3a, lower and middle panels; Fig. 3b). A second possibility is that under hypoxic conditions there may be differences in the expression and phosphorylation state of Max, which forms a heterodimer with Myc, as well as differences in the phosphorylation state of Myc itself. Both N-Myc and c-Myc form a heterodimer with Max, and this complex can bind to the E-box [2,4,6,30], and regulate HMGA1a [43]. Moreover, many phosphorylation sites on these proteins are known, and these functions are intricately regulated by phosphorylation [9–12,14–17,26,27,33,34,40,42]. It is unclear which functions are required under hypoxia, but precise functional regulation through expression and/or phosphorylation of Max and the level of post-translational modification of Myc family members may lead to PS2V expression in neuroblastoma cell lines such as SK-N-SH cells, but not in 293T and HeLa cells. We note that hypoxia stimulation of SK-N-SH cells led to changes in the phosphorylation of N-Myc, which strongly supports this hypothesis.

As mentioned above, there is accumulating evidence that phosphorylation of the N-Myc protein at serine and/or threonine residues indeed occurs in response to a variety of intracellular signals [10,17]. Furthermore, phosphorylation of the N-Myc protein at Ser-51 by MAP kinase is required for the transcriptional repression activity of the protein [17]. However, the present immunoprecipitation analysis clearly demonstrated phosphorylation of the N-Myc protein at tyrosine residues after 8 h of hypoxia (Fig. 5a). Although the exact molecular mechanism and functional significance are not yet clear, this is the first direct demonstration of phosphorylation of tyrosine residues of N-Myc in nuclear fractions, in response to a particular extracellular signal. N-Myc is a 456-amino acid protein that contains five tyrosine residues at positions 21, 28, 324, 330 and 421. Serine and threonine phosphorylation in N-Myc is more likely than tyrosine phosphorylation in the initial response to hypoxia. However, phosphorylation of tyrosines, as well as of serines and threonines, could play a crucial role underlying subsequent consolidation of extracellular signals due to hypoxia, through modulation of the transcriptional activity of the Myc/Max complex in neuroblastoma cell lines. However, phosphorylation of Myc family members other than N-Myc was not confirmed in the present study.

In conclusion, our results suggest that differences in expression and in the phosphorylation state of Myc proteins occur in response to a hypoxic stimulus, and that these in part cause induction of HMGA1a and subsequent generation of PS2V, which in turn has aberrant effects on the nervous system.

References

[1] Y. Azuma, K. Ogita, Y. Yoneda, Particular nuclear transcription factors responsive to systemic administration of kainic acid in murine brain, Neurochem. Int. 29 (1996) 289–299.

[2] N. Benvenisty, D.M. Ornitz, G.L. Bennett, B.G. Sahagan, A. Kuo, R.D. Cardiff, P. Leder, Brain tumours and lymphomas in transgenic mice that carry HTLV-I LTR/c-myc and Ig/tax genes, Oncogene 7 (1992) 2399–2405.

[3] O. Bernard, J. Drago, H. Sheng, L-myc and N-myc influence lineage determination in the central nervous system, Neuron 9 (1992) 1217–1224.

[4] E. Blackwood, R.N. Eisenman, Max: a helix–loop–helix zipper protein that forms a sequence-specific DNA-binding complex with Myc, Science 251 (1991) 1211–1217.

[5] M.D. Cole, S.B. McMahon, The Myc oncoprotein: a critical evaluation of transactivation and target gene regulation, Oncogene 18 (1999) 2916–2924.

[6] M. Eilers, S. Schirm, J.M. Bishop, The MYC protein activates transcription of the alpha-prothymosin gene, EMBO J 10 (1991) 133–141.

[7] I. Ferrer, R. Blanco, N-myc and c-myc expression in Alzheimer disease, Huntington disease and Parkinson disease, Brain Res. Mol. Brain Res. 77 (2000) 270–276.

[8] I. Ferrer, R. Blanco, M. Carmona, B. Puig, Phosphorylated c-MYC expression in Alzheimer disease, Pick's disease, progressive supranuclear palsy and corticobasal degeneration, Neuropathol. Appl. Neurobiol. 27 (2001) 343–351.

[9] S. Gupta, A. Seth, R.J. Davis, Transactivation of gene expression by Myc is inhibited by mutation at the phosphorylation sites Thr-58 and Ser-62, Proc. Natl. Acad. Sci. U.S.A. 90 (1993) 3216–3220.

[10] T. Hagiwara, K. Nakaya, Y. Nakamura, H. Nakajima, S. Nishimura, Y. Taya, Specific phosphorylation of the acidic central region of the N-myc protein by casein kinase II, Eur. J. Biochem. 209 (1992) 945–950.

[11] M. Henriksson, A. Bakardjiev, G. Klein, B. Luscher, Phosphorylation sites mapping in the N-terminal domain of c-myc modulate its transforming potential, Oncogene 8 (1993) 3199–3209.

[12] A.T. Hoang, B. Lutterbach, B.C. Lewis, T. Yano, T.Y. Chou, J.F. Barrett, M. Raffeld, S.R. Hann, C.V. Dang, A link between increased transforming activity of lymphoma-derived MYC mutant alleles, their defective regulation by p107, and altered phosphorylation of the c-Myc transactivation domain, Mol. Cell. Biol. 15 (1995) 4031–4042.

[13] B. Hoffman, D.A. Liebermann, The proto-oncogene c-myc and apoptosis, Oncogene 17 (1998) 3351–3357.

[14] B. Lutterbach, S.R. Hann, Hierarchical phosphorylation at N-terminal transformation-sensitive sites in c-Myc protein is regulated by mitogens and in mitosis, Mol. Cell. Biol. 14 (1994) 5510–5522.

[15] B. Lutterbach, S.R. Hann, Overexpression of c-Myc and cell immortalization alters c-Myc phosphorylation, Oncogene 14 (1997) 967–975.

[16] B. Lutterbach, S.R. Hann, c-Myc transactivation domain-associated kinases: questionable role for map kinases in c-Myc phosphorylation, J. Cell Biochem. 72 (1999) 483–491.

[17] A. Manabe, S.M. Iguchi-Ariga, H. Iizuka, H. Ariga, Transcriptional repression activity of N-MYC protein requires phosphorylation by MAP kinase, Biochem. Biophys. Res. Commun. 219 (1996) 813–823.

[18] T. Manabe, T. Kitayama, K. Ogita, Y. Yoneda, Differential expression and phosphorylation of particular Fos family members by kainate in nuclear and cytosolic fractions of murine hippocampus, Neuroscience 100 (2000) 453–463.

[19] T. Manabe, T. Katayama, N. Sato, F. Gomi, J. Hitomi, T. Ynagita, T. Kudo, A. Honda, Y. Mori, K. Imaizumi, A. Mayeda, M. Tohyama, Induced HMGA1a expression causes aberrant splicing of presenilin-

2 pre-mRNA in sporadic Alzheimer's disease, Cell Death Differ. 10 (2003) 698–708.
[20] T. Manabe, T. Katayama, N. Sato, T. Kudo, S. Matsuzaki, K. Imaizumi, M. Tohyama, The cytosolic inclusion bodies that consists of splice variants that lack exon 5 of the presenilin-2 gene differ obviously from Hrano bodies observed in the brain from sporadic cases of Alzheimer's disease patients, Neurosci. Lett. 323 (2002) 198–200.
[21] T. Manabe, N. Kuramoto, N. Nakamichi, K. Aramachi, K. Baba, T. Hirai, M. Yoneyama, Y. Yoneda, Degradation of c-Fos protein expressed by *N*-methyl-D-aspartic acid in nuclear fractions of murine hippocampus., Brain Res. 905 (2001) 34–43.
[22] T. Manabe, K. Ogita, N. Nakamichi, Y. Yoneda, Differential in vitro degradation of particular Fos family members expressed by kainic acid in nuclear and cytosolic fractions of murine hippocampus, J. Neurosci. Res. 64 (2001) 34–42.
[23] L. McGahan, A.M. Hakim, G.S. Robertson, Hippocampal Myc and p53 expression following transient global ischemia, Brain Res. Mol. Brain Res. 56 (1998) 133–145.
[24] T. Nakagomi, A. Asai, H. Kanemitsu, K. Narita, Y. Kuchino, A. Tamura, T. Kirino, Up-regulation of c-myc gene expression following focal ischemia in the rat brain, Neurol. Res. 18 (1996) 559–563.
[25] A. Nisikawa, T. Manabe, T. Katayama, T. Kudo, S. Matsuzaki, T. Yanagita, H. Okuda, Y. Bando, M. Tohyama, Novel function of PS2V: change in conformation of tau proteins, Biochem. Biophys. Res. Commun. 318 (2004) 435–438.
[26] K. Noguchi, C. Kitanaka, H. Yamana, A. Kokubu, T. Mochizuki, Y. Kuchino, Regulation of c-Myc through phosphorylation at Ser-62 and Ser-71 by c-Jun N-terminal kinase, J. Biol. Chem. 274 (1999) 32580–32587.
[27] N. Nozaki, T. Naoe, T. Okazaki, Immunoaffinity purification and characterization of CACGTG sequence-binding proteins from cultured mammalian cells using an anti c-Myc monoclonal antibody recognizing the DNA-binding domain, J. Biochem. (Tokyo) 121 (1997) 550–559.
[28] A.J. Obaya, M.K. Mateyak, J.M. Sedivy, Mysterious liaisons: the relationship between c-Myc and the cell cycle, Oncogene 18 (1999) 2934–2941.
[29] G.C. Prendergast, Mechanisms of apoptosis by c-Myc, Oncogene 18 (1999) 2967–2987.
[30] G.C. Prendergast, D. Lawe, E.B. Ziff, Association of Myn, the murine homolog of Max with c-Myc stiumulates methylation-sensitive DNA binding and Ras cotransformation, Cell 65 (1991) 395–407.
[31] R. Reeves, Molecular biology of HMGA proteins: hubs of nuclear function, Gene 277 (2001) 63–81.
[32] J. Rossler, M. Schwab, W. Havers, L. Schweigerer, Hypoxia promotes apoptosis of human neuroblastoma cell lines with enhanced N-myc expression, Biochem. Biophys. Res. Commun. 281 (2001) 272–276.
[33] K. Saksela, T.P. Makela, G. Evan, K. Alitalo, Rapid phosphorylation of the L-myc protein induced by phorbol ester tumor promoters and serum, EMBO J. 8 (1989) 149–157.
[34] K. Saksela, T.P. Makela, K. Hughes, J.R. Woodgett, K. Alitalo, Activation of protein kinase C increases phosphorylation of the L-myc trans-activator domain at a GSK-3 target site, Oncogene 7 (1992) 347–353.
[35] N. Sato, O. Hori, A. Yamaguchi, J.C. Lambert, M.C. Chartier-Harlin, P.A. Robinson, A. Delacourte, A.M. Schmidt, T. Furuyama, K. Imaizumi, M. Tohyama, T. Takagi, A novel presenilin-2 splice variant in human Alzheimer's disease brain tissue, J. Neurochem. 72 (1999) 2498–2505.
[36] N. Sato, K. Imaizumi, T. Manabe, M. Taniguchi, J. Hitomi, T. Katayama, T. Yoneda, T. Morihara, Y. Yasuda, T. Takagi, T. Kudo, T. Tsuda, Y. Itoyama, T. Makifuchi, P.E. Fraser, P. St George-Hyslop, M. Tohyama, Increased production of b-amyloid and vulnerability to ER stress by an aberrant spliced form of presenilin-2, J. Biol. Chem. 276 (2001) 2108–2114.
[37] S. Sawai, A. Shimono, Y. Wakamatsu, C. Palmes, K. Hanaoka, H. Kondoh, Defects of embryonic organogenesis resulting from targeted disruption of the N-myc gene in the mouse, Development 117 (1993) 1445–1455.
[38] E. Schreiber, P. Matthias, M.M. Muller, W. Schaffner, Rapid detection of octamer binding proteins with 'mini-extracts', prepared from a small number of cells, Nucleic Acids Res. 17 (1989) 6419.
[39] D.J. Selkoe, Normal and abnormal biology of the beta-amyloid precursor protein, Annu. Rev. Neurosci. 17 (1994) 489–517.
[40] A. Seth, E. Alvarez, S. Gupta, R.J. Davis, A phosphorylation site located in the NH2-terminal domain of c-Myc increases transactivation of gene expression, J. Biol. Chem. 266 (1991) 23521–23524.
[41] Y. Wakamatsu, Y. Watanabe, H. Nakamura, H. Kondoh, Regulation of the neural crest cell fate by N-myc: promotion of ventral migration and neuronal differentiation, Development 124 (1997) 1953–1962.
[42] A. Wenzel, C. Cziepluch, U. Hamann, J. Schurmann, M. Schwab, The N-Myc oncoprotein is associated in vivo with the phosphoprotein Max(p20/22) in human neuroblastoma cells, EMBO J. 10 (1991) 3703–3712.
[43] L.J. Wood, M. Mukherjee, C.E. Dolde, Y. Xu, J.F. Maher, T.E. Bunton, J.B. Williams, L.M. Resar, HMG-I/Y, a new c-Myc target gene and potential oncogene, Mol. Cell. Biol. 20 (2000) 5490–5502.
[44] Y. Yoneda, K. Ogita, Y. Azuma, M. Ikeda, H. Tagami, T. Manabe, *N*-Methyl-D-aspartate signaling to nuclear activator protein-1 through mechanisms different from those for kainate signaling in murine brain, Neuroscience 90 (1999) 519–533.
[45] Y. Yoneda, K. Ogita, Y. Azuma, N. Kuramoto, T. Manabe, T. Kitayama, Predominant expression of nuclear activator protein-1 complex with DNA binding activity following systemic administration of *N*-methyl-D-aspartate in dentate granule cells of murine hippocampus, Neuroscience 93 (1999) 19–31.

Journal of Neurochemistry, 2004, **88**, 1345–1351 doi:10.1111/j.1471-4159.2004.02290.x

Metals accelerate production of the aberrant splicing isoform of the presenilin-2

Shinsuke Matsuzaki,*,† Takayuki Manabe,*,† Taiichi Katayama,*,† Atsuko Nishikawa,*,† Takeshi Yanagita,*,† Hiroaki Okuda,*,† Yuichi Yasuda,*,†,‡ Shingo Miyata,*,† Shunsuke Meshitsuka§ and Masaya Tohyama*,†

**Department of Anatomy and Neuroscience, Osaka University Graduate School of Medicine, Osaka, Japan*

†CREST of Japan Science and Technology Corporation (JST), Kawaguchi, Saitama, Japan

‡Sysmex Corporation, Kobe, Japan

§Department of Biochemical Science, Tottori University Graduate School of Medical Science, Yonago, Tottori, Japan

Abstract

Oxidative stress is a major risk factor for Alzheimer's disease (AD) and other neurodegenerative disorders. Metals are known to be one of the factors that contribute to oxidative stress. Recently, we reported that the aberrant splicing isoform (PS2V) generated by skipping exon5 of the presenilin-2 (PS2) gene is a diagnostic feature of sporadic AD (SAD). PS2V is inducible by exposure of human neuroblastoma to hypoxia. We examined whether this aberrant splicing was caused by metal-induced oxidative stress, such as exposure to aluminum. As a result, we demonstrated that exposure to aluminum accelerated PS2V production induced by hypoxia. This acceleration of the production of PS2V to hypoxia was caused by chronic aluminum exposure, but was not related to the intracellular content of aluminum. HMGA1a is a mediator of PS2V production, and it was induced by aluminum as well as by hypoxia. Induction of HMGA1a was increased by chronic exposure to aluminum, and a nuclear extract containing HMGA1a bound to a specific sequence on exon5 of PS2 pre-mRNA, as reported previously. Finally, the acceleration of PS2V production induced by aluminum under hypoxic conditions reflected, but has not yet been directly shown to cause, vulnerability to endoplasmic reticulum stress. These results suggest that exposure to some metals can accelerate and enhance PS2V generation, and that hypoxia plus chronic exposure to metals may promote the development of AD.

Keywords: Alzheimer's disease, HMGA1a, hypoxia, metal, presenilin 2, splicing.

J. Neurochem. (2004) **88**, 1345–1351.

Alzheimer's disease (AD) is a neurodegenerative disorder that is clinically characterized by progressive loss of memory and other cognitive abilities, and pathologically features severe neuronal loss, glial proliferation, extracellular senile plaques composed of amyloid-β protein (Aβ), and intraneuronal neurofibrillary tangles (reviewed in Selkoe 1994). In early onset forms of AD, some of these changes are caused by abnormalities of the amyloid precursor protein (APP) gene located on chromosome 21 as well as presenilin genes 1 and 2 located on chromosomes 14 and 1, respectively (Goate *et al.* 1991; Rogaev *et al.* 1995). Despite extensive research, however, little is known about the mechanisms that underlie sporadic AD, which accounts for over 90% of all cases of this disease.

Recently, we reported the preferential expression of a characteristic splicing variant of the PS2 gene that lacks exon 5 (an isoform termed PS2V) in sporadic AD brains, which was not caused by a mutation of the gene but possibly by a *trans*-acting factor (Sato *et al.* 1999). We showed that PS2V protein impaired the signaling pathway of the unfolded protein response (UPR), in a manner similar to familial AD-linked PS1 mutant proteins, and caused a significant increase in the

Resubmitted manuscript received October 10, 2003; accepted October 28, 2003.

Address correspondence and reprint requests to Taiichi Katayama, Department of Anatomy and Neuroscience, Osaka University Graduate School of Medicine. 2–2, Yamada-oka, Suita, Osaka 565–0871, Japan. E-mail: katayama@anat2.med.osaka-u.ac.jp

Abbreviations used: Aβ, amyloid-β protein; AD, Alzheimer's disease; Al-maltol, aluminum maltolate; APP, amyloid precursor protein; HMGA1a, high mobility group A1a protein; PS2, presenilin-2; ROS, reactive oxygen species; SAD, sporadic Alzheimer's disease; SDS–PAGE, sodium dodecyl sulfate–polyacrylamide gel electrophoresis; Tm, tunicamycin; UPR, unfolded protein response.

production of Aβ protein (Katayama *et al.* 1999; Sato *et al.* 1999). Interestingly, PS2V-encoded aberrant proteins were observed in vulnerable pyramidal cells of the hippocampal CA1 region as well as in cells of the cerebral cortex in sporadic AD brains (Sato *et al.* 2001; Manabe *et al.* 2002). Furthermore, we found that PS2V could be induced in human neuroblastoma SK-N-SH cells by exposure to hypoxia and purified the responsible *trans*-acting factor based on its binding to an exon 5 fragment. As a result, high mobility group A1a protein (HMGA1a; formerly known as HMG-I) was identified as the factor (Manabe *et al.* 2003). The expression of HMGA1a was induced by hypoxia and subsequently led to the generation of PS2V (Manabe *et al.* 2003). In addition, the finding that antioxidants inhibited generation of the hypoxia-induced splice variant suggests that even at a low oxygen tension (8 Torr)(Sato *et al.* 1999), oxidative stress and the production of reactive oxygen species (ROS) may occur and with various deleterious effects (Borgern and Essig 1998). Indeed, recent studies have suggested that enhanced cellular oxidative stress may contribute to the progressive neurodegeneration that is observed in AD.

Metals play a major catalytic role in the production of free radicals, and attention has been paid to the role of various metals in AD, including iron, aluminum, copper, and zinc (Bush 2003). Iron is involved in the formation of free radicals, which have well-known deleterious effects, via the classical Fenton and Haber–Weiss reactions. Many observations have yielded evidence that iron metabolism is involved in AD (Loeffler *et al.* 1995; Kennard *et al.* 1996; Markesbery 1997; Smith *et al.* 1997). For example, the concentration of iron is elevated in the brains of AD patients, while iron, transferrin, and ferritin have all been found in senile plaque (Loeffler *et al.* 1995; Markesbery 1997). It was reported that copper can act as a catalyst in the production of ROS and it has been shown that the APP molecule contains a copper-binding site (Multhaup *et al.* 1996, 1998; Multhaup 1997; White *et al.* 2001). Moreover, copper is essential for the activity of enzymes, including cytochrome-c oxidase and Cu/Zn superoxide dismutase (Curtain *et al.* 2001; Linder and Hazegh-Azam 1996). Aluminum is thought to have a weaker effect on the formation of free radicals, but it has also been suggested as one of the causative factors involved in the onset of AD (Crapper *et al.* 1980; Pratico *et al.* 2002).

Here, we investigated whether aberrant splicing (production of PS2V protein) was caused by metal-induced oxidative stress, especially by exposure to aluminum at low concentrations that did not have a neurotoxic effect.

Materials and methods

Cell culture

Human neuroblastoma SK-N-SK cells were maintained in α-MEM supplemented with 10% heat-inactivated fetal bovine serum (Sigma, St Louis, MO, USA), as described previously (Manabe *et al.* 2003).

Preparation of aluminum maltolate

Aluminum maltolate (Al-maltol) was prepared from aluminum potassium sulfate dodecahydrate (Sigma-Aldrich/Katayama Chemical. Inc., Osaka, Japan) and maltol (3-hydroxy-2-methyl-4-pyron)(Sigma-Aldrich/Katayama Chemical. Inc., Osaka, Japan), as described previously (Finnegan *et al.* 1986).

Exposure to Al-maltol and hypoxia

Culture of cells and exposure to hypoxia were performed as described previously (Manabe *et al.* 2003). For short-term exposure to Al-maltol, SK-N-SH cells were treated with 2.5–250 μM Al-maltol for 21 h. For chronic exposure, cells were treated with 2.5 or 25 μM Al-maltol for 3 months. As a control, cells were exposed to maltol alone and untreated control cells were also prepared.

Aluminum quantitation

Cell pellets were freeze-dried, and then atomic absorbance spectrometry was used to measure the aluminum content (Meshitsuka and Inoue 1998; Meshitsuka *et al.* 1999)

Preparation of total RNA and RT-PCR

Preparation of total RNA from neuroblastoma SK-N-SH cells and RT-PCR were performed as described previously (Sato *et al.* 1999) with minor modifications. Reverse transcription was carried out using Moloney murine leukemia virus (M-MLV) reverse transcriptase (Promega, Madison, WI, USA). The PCR conditions were described previously (Sato *et al.* 1999). Experiments were repeated at least four times using separate cell cultures and consistent results were obtained in all cases.

Preparation of nuclear extracts and nuclear fraction

Nuclear extracts and nuclear fractions were prepared from cultured cell lines as described elsewhere (Schreiber *et al.* 1989) with minor modifications (Yoneda *et al.* 1999; Manabe *et al.* 2000).

Preparation of RNA probes

RNA probes [including the no.5 probe (41nt)] were prepared by *in vitro* transcription with DNA template constructs (Manabe *et al.* 2003) in pcDNA3 vectors (Invitrogen, Carlsbad, CA, USA), as described previously (Manabe *et al.* 2003). In brief, the template plasmid (linearized with EcoRI) was incubated for 1 h at 37°C in a transcription reaction mixture (20 μL) containing 0.5 mM ATP, 0.5 mM CTP, 0.5 mM GTP, 0.25 mM UTP, [^{35}S]UTPαS, 40 units of RNase inhibitor (TOYOBO, Tokyo, Japan), and 20 units of T7 RNA polymerase with the reaction buffer provided by the manufacturer (Promega).

UV cross-linking assays

The UV cross-linking assay was also described previously (Manabe *et al.* 2003). Briefly, an aliquot of nuclear extract (estimated protein content: 5 μg) was incubated for 30 min at 25°C in 25 μL of incubation buffer [12 mM HEPES–NaOH (pH 7.9), 60 mM KCl, 4 mM $MgCl_2$, 1 mM EDTA, 1 mM EGTA, 1 mM dithiothreitol, 10% glycerol, and 1 mM phenylmethylsulfonyl fluoride] with 10 μg of tRNA and a ^{35}S-labeled RNA probe (1 μg). This reaction mixture

was irradiated with UV light (254 nm, 60 W) for 15 min at room temperature. Free probes were digested at 25°C for 30 min with 10 μg of RNase A, followed by the addition of a four-fold volume of sodium dodecyl sulfate–polyacrylamide gel electrophoresis (SDS–PAGE) sample dye mixture [10 mM Tris-HCl (pH 6.8), 10% glycerol, 2% SDS, 0.01% bromophenol blue and 5% 2-mercaptoethanol]. After separation by SDS–PAGE on 15% polyacrylamide gel, the gel was fixed, dried, and analyzed with a Bio Imaging Analyzer (BAS-5000; Fujifilm Medical Systems). Each experiment was repeated at least three times using separate cell cultures and consistent results were obtained in all cases.

Immunoblotting assay

Immunoblotting was performed as described previously (Manabe *et al.* 2001a, 2001b) with minor modifications. Anti-HMGA1 [HMG-I(Y) (N-19)] goat polyclonal antibody was purchased from Santa Cruz Biotechnology (Santa Cruz, CA, USA) for this assay.

Cell death assay

To estimate the vulnerability of cells, cell death was assessed on the basis of morphological changes observed by phase contrast microscopy or nuclear changes detected by fluorescence microscopy after costaining the cells with 10 μM Hoechst 33342 and 10 μM propidium iodide. That is, nuclear fragmentation was detected by Hoechst-positive staining and nuclear membrane collapse was detected by propidium iodide-positive staining. We determined dead cells by the above double positive. The staining was measured independently in 10 fields and at least 500 cells were counted, and the data was expressed as the mean ± SEM for three independent experiments. The percentage (%) of dead cells was calculated after each treatment relative to control cultures.

Results

Transient exposure to various metals

First, we examined the production of PS2V when SK-N-SH neuroblastoma cells were exposed to various metals. PS2V was produced after exposure of the cells to $FeCl_2$, $FeCl_3$, $ZnCl_2$, $CuCl_2$, $CuSO_4$, $AlCl_3$, and Al-maltol (Fig. 1a). However, the level of PS2V production was not consistent between experiments using a given concentration of metal, except in the case of aluminum, since addition of $AlCl_3$ and Al-maltol resulted in the reproducible production of PS2V (Fig. 1a). Accordingly, we performed the following experiments using Al-maltol as the test metal.

As shown in Fig. 1, expression of PS2V was increased by about 12-fold after exposure to hypoxia for 24 h (Fig. 1b, control), consistent with our previous report. Exposure to Al-maltol at a concentration of 25 or 250 μM also caused the production of PS2V without any exposure to hypoxia. Furthermore, exposure to Al-maltol promoted the production of PS2V at 12 h after hypoxia even when PS2V was not induced by hypoxia alone (Fig. 1b, squares). Although the promotion of PS2V production was also seen at 24 h after hypoxia followed by exposure to Al-maltol at a concentration of 25 μM, Al-maltol at a concentration of 250 μM caused a decrease to control levels of PS2V thereafter (Fig. 1b).

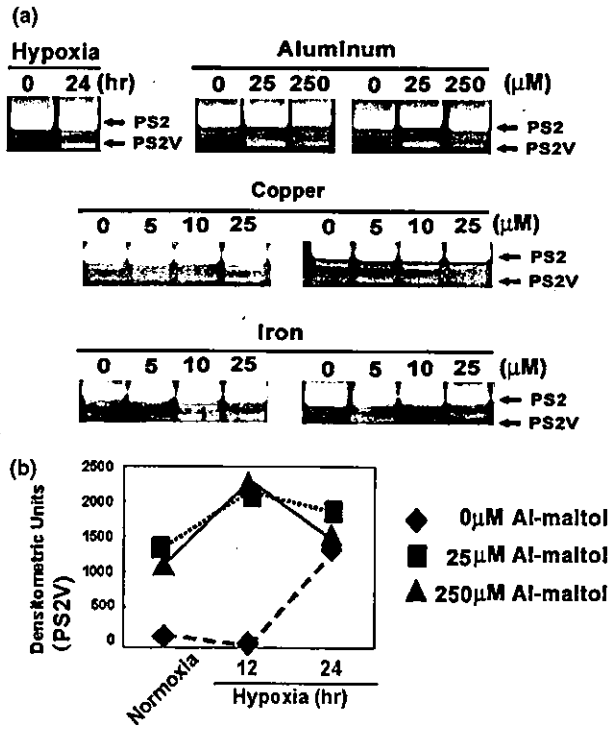

Fig. 1 Effect of metals on the expression of PS2V in SK-N-SH cells. (a) RT-PCR-amplified products were separated on a polyacrylamide gel and visualized by ethidium bromide staining. Arrows indicate the positions of the normal PS2 transcript and the aberrant PS2V transcript. Total RNA was extracted from the cells exposed to indicated metals (Al-mal, aluminum; $CuCl_2$, copper; $FeCl_2$, Iron) or hypoxia-exposed cells. Each column shows the independent experimental data. (b) Effect of short-term incubation with Al-maltol on hypoxia-induced expression of PS2V. Cells were incubated without Al-maltol (rhomboids) or with 25 μM (■) or 250 μM (▲) Al-maltol for 24 h, followed by hypoxic stimulation. The cells were harvested at 0–24 h after hypoxic stimulation and total RNA was prepared for RT-PCR of PS2V. Quantitative data were obtained by densitometry of the band corresponding to the molecular weight of PS2V (shown as a percentage of control).

Chronic exposure to a low concentration of Al-maltol

Next, we examined the effect of chronic exposure to a low concentration of Al-maltol on the hypoxia-induced expression of PS2V in SK-N-SH cells. As shown in Fig. 2, there was no significant expression of PS2V when SK-N-SH cells were exposed to 2.5 μM or 25 μM Al-maltol for 3 months under normoxic conditions (Fig. 2, normoxia). On the other hand, hypoxia of 0.5 h or more caused a significant increase of PS2V expression in SK-N-SH cells exposed to 2.5 μM or 25 μM Al-maltol for 3 months. This potentiation by hypoxia was maximal over a period of 4 h and persisted for at least 8 h (Fig. 2). However, aluminum

